# State of the Art and Challenges of the ab Initio Theory of Intermolecular Interactions

Grzegorz Chałasiński*,†

*Department of Chemistry, University of Warsaw, Pasteura 1, 02–093 Warszawa, Poland*

Małgorzata M. Szczęśniak*,‡

*Department of Chemistry, Oakland University, Rochester, Michigan 48309*

*Received February 3, 2000*

## Contents



† Phone: 48-22-8222309. Fax: 48-22-8222309. E-mail: chalbie@chem.uw.edu.pl.
‡ Phone: 248−3702087. Fax: 248−3702321. E-mail: maria@ouchem.chem.oakland.edu.

## I. Introduction

The past decade has seen explosive growth in experimental and theoretical studies of van der Waals interactions. Considerable progress has been achieved toward understanding the nature of these interactions at the fundamental level. Ab initio theory has played a central role in this progress. The earlier applications of ab initio techniques to this problem concentrated primarily on the qualitative understanding of these interactions. These applications greatly benefited from the partitioning of interaction energy into its fundamental components, such as electrostatic, exchange, induction, and dispersion. The analyses of a large number of model complexes helped to identify the origins of binding and the sources of anisotropy of these interactions. A detailed examination of the interaction energy components and their computational requirements shed new light on the question of how to saturate the basis-set and the correlation effects. Progress in computational capabilities enabled the use of sufficiently large basis sets and highly correlated methods. With the background of these advances, the ab initio theory of intermolecular interactions entered a new quantitative phase. The progress in the accurate predictions of potential-energy surfaces for these interactions has been matched by new treatments of multidimensional fully coupled vibration dynamics, thereby establishing a direct connection to experimental observations.

*Chemical Reviews* helped sort out these advances by periodically revisiting the topic of van der Waals interactions. In 1994, in the "van der Waals Molecules II" issue,[1] contributors, including ourselves, laid out the then state of the art of the post-Hartree−Fock theory of van der Waals interactions.[2−5] These

10.1021/cr990048z CCC: $35.00 
Published on Web 10/12/2000

Grzegorz Chałasiński is a Professor at Warsaw University, Chemistry Department, Warsaw, Poland. He has been with the Chemistry Department of Warsaw University since 1972, where he obtained his M.S. degree (1972) and Ph.D. (1977) degree and was appointed as a Professor in 1986. During that time, he spent one year as a visiting professor at the University of Utrecht, Holland (1979), and two years as a postdoctoral fellow at the University of Utah (1985–87). Since 1989 he has collaborated with the Departments of Chemistry of Southern Illinois University and Oakland University. His primary research interests include the theory of intermolecular interactions and ab initio calculations of the electronic structure of van der Waals clusters. Perturbation analysis of the supermolecular method in calcualtions of the interaction energies and elucidating of the origin of the basis-set superposition error are among his most important achievements.

Malgorzata M. Szczęśniak was born in Wroclaw, Poland. She received her M.S. degree from the University of Wroclaw in 1973. In 1978 she received her Ph.D. degree from the University of Wroclaw. She was a postdoctoral fellow (1981–1983) with Professor Steve Scheiner at Southern Illinois University at Carbondale. She held a Visiting Assistant Professor position (1983–1989) and an Associate Research Professor (1989–1991) at SIU. In 1991 she joined the faculty of Oakland University in Rochester, MI, where she is now Professor of Chemistry.

contributions demonstrated that the supermolecular approach based on the Møller−Plesset perturbation and coupled-cluster theories, along with the symmetry-adapted perturbation theory, is capable of providing the rigorous, quantitative, and physically meaningful description of intermolecular forces. It was shown that these approaches ultimately provide accurate and complete intermolecular potential-energy surfaces. The ab initio theory of many-body effects was also addressed.[2] The contributions[2−5] were amply illustrated by calculations performed for a number of van der Waals clusters. These topics were further elaborated in recent monographs edited by Scheiner[6] and Hadži.[7]

Since 1994, the methods and techniques recommended in the last issue "van der Waals Molecules II" have been perfected and mastered. Today, the calculations of reliable potential-energy surfaces for small clusters composed of closed-shell species, atoms, and rigid molecules have become fairly straightforward.[2−7] The collaboration between theory and experiment has served as an extremely rich source of information on the dynamics of these complexes. It is thus worthwhile to revisit the recent progress in this field in the present review. In the first part, the current state of the ab initio theory of van der Waals interactions will be discussed, which may be thought of as a supplement to our previous review.[2] The spectacular successes in ab initio predictions of the energetics and dynamics of closed-shell dimers will be presented. New methodological developments, such as density functional theory (DFT) and local-correlation methods, which open up the possibility of applications to larger systems, will also be discussed.

In the second part of this review some persisting challenges, as well as new avenues, will be presented which, in our opinion, set the stage for ab initio research soon. The themes which have already been dealt with previously, but not yet resolved satisfactorily, include (i) accounting for the intramonomer relaxation and (ii) some issues pertaining to many-body effects. The new avenues contain the interactions with open-shell monomers. Such interactions are interesting as intermediate between van der Waals and chemical interactions.[8] More importantly, these complexes frequently precede a chemical reaction and hence determine the subsequent fate of a reaction itself.[9,10] They also introduce us to an even less-traveled area of intermolecular interactions involving manifolds of potential surfaces and to the issues of the spin−orbit coupling.[11,12] Ab initio calculations of such interactions often demand a consideration of multireference correlation techniques for which the problems of basis-set superposition error, size consistency, nonadiabatic effects, and spin−orbit coupling represent a serious challenge.

## *II. State of the Art*

### A. General Outline of the Supermolecular Approach

The total binding energy of a trimer in which the monomers are subjected to geometrical relaxation may be written as follows, cf., e.g., refs 4 and 13

$$\Delta E(\text{cluster}) = \Delta E(\text{1-body}) + \Delta E(\text{2-body}) + \Delta E(\text{3-body}) + ... + \Delta E(N\text{-body}) \quad (1)$$

where $\Delta E$(1-body) collects the distortion energies of monomers in the trimer and $\Delta E$(2-body) represents the two-body, $\Delta E$(3-body) the three-body, and $\Delta E$($N$-body) the $N$-body interaction energies among the relaxed monomers. Upon inclusion of the explicit dependence on all inter- and intramonomer geometrical parameters in every term of eq 1, one recovers the full cluster potential-energy surface, suitable for performing many-dimensional dynamics calculations. The binding energy, as defined in eq 1,

**Table 1. Decomposition of Two- and Three-Body Supermolecular (S-MP) Interaction Energies[a]**

| S-MP | SAPT | physical interpretation |
|---|---|---|
| | | Two-body |
| $\Delta E^{SCF}$ | $\epsilon_{es}^{(10)}$ | electrostatic energy between SCF monomers |
| | $\epsilon_{exch}^{HL}$ | exchange repulsion between SCF monomers |
| | $\Delta E^{delSCF}$ | mutual polarization restrained by exchange [$\epsilon_{ind,r}^{(20)}$] |
| $\Delta E^{(2)}$ | $\epsilon_{disp}^{(20)}$ | dispersion energy arising between SCF monomers (second order). |
| | $\epsilon_{es,r}^{(12)}$ | electrostatic−correlation energy (second order) i.e., intramonomer correlation correction to $\epsilon_{es}^{(10)}$ |
| | $\Delta E_{def}^{(2)}$ | 1. deformation−intracorrelation [$\epsilon_{ind,r}^{(22)}$] |
| | | 2. deformation−dispersion [$\epsilon_{disp-ind}^{(30)}$] |
| | $\Delta E_{exch}^{(2)}$ | 1. exchange−dispersion [$\epsilon_{exch-disp}^{(20)}$] |
| | | 2. exchange−intracorrelation |
| | $\Delta E^{(3)}$, $\Delta E^{(4)}$, etc. | higher-order correlation corrections to the terms described for $\Delta E^{(2)}$ |
| | | Three-body |
| $\Delta E^{SCF}$ | $\epsilon_{exch}^{HL}$ | 1. SE component: single exchanges between monomers |
| | | 2. TE component: all monomers are involved in the exchange |
| | $\Delta E_{def}^{SCF}$ | SCF-deformation nonadditivity [$\epsilon_{ind,r}^{(20)}$, $\epsilon_{ind,r}^{(30)}$] |
| $\Delta E^{(2)}$ | | 1. exchange−dispersion nonadditivity [$\epsilon_{exch-disp}^{(20)}$] |
| | | 2. exchange−intracorrelation nonadditivity |
| | | 3. deformation−intracorrelation nonadditivity [$\epsilon_{ind,r}^{(22)}$] |
| | | 4. deformation−dispersion nonadditivity [$\epsilon_{disp-ind}^{(30)}$] |
| $\Delta E^{(3)}$ | $\epsilon_{disp}^{(30)}$ | dispersion nonadditivity related to Axilrod−Teller−Muto |
| | | higher-order correlation corrections to the terms described for $\Delta E^{(2)}$ |
| $\Delta E^{(4)}$, etc. | | higher-order correlation corrections to the terms described for $\Delta E^{(3)}$ |

[a] The contents of S-MP terms are described in terms of SAPT $\epsilon^{(ij)}$ corrections (where $i$ and $j$ correspond to the interaction and the intramonomer correlation operators, respectively) shown in square brackets.

encompasses the total energetic effect of the interaction. The $\Delta E$(cluster) energy is sometimes referred to as the interaction energy, but it has recently been argued that, strictly speaking, one should apply this name only to the sum of the second, third, ..., $N$th term on the right-hand side of eq 1.[4,14]

Equation 1 defines the binding energy as the difference between the fully geometry-optimized cluster and free, undistorted monomers. Hence, the distortion of monomers, $\Delta E$(1-body), is always a repulsive effect, whereas the stabilization of the cluster is provided primarily by the two-body part and additionally by cooperative many-body terms. The change in the monomer geometries occurs when the stabilization gain of the two-body and many-body interactions under distortion is larger than the destabilizing one-body term. This balance may be a subtle one, and thus geometry optimization of van der Waals complexes must be accompanied by the careful monitoring of errors, in particular correcting the basis-set superposition error (BSSE) with the aid of the counterpoise correction (CP).[15] The procedure to follow has been described, e.g., by van Duijneveldt[16] and recently applied by Xantheas,[17] Simon et al.,[18] and Hobza et al.[19] It consists of performing the optimization on the CP-corrected surface.

The energies appearing in eq 1 can be evaluated at any level of a size-consistent method. In the framework of supermolecular Møller−Plesset (MP) perturbation theory, eq 1 may be written as

$$\Delta E^{(n)}(\text{cluster}) = \Delta E^{(n)}(\text{1-body}) + \Delta E^{(n)}(\text{2-body}) + \Delta E^{(n)}(\text{3-body}) + ... + \Delta E^{(n)}(N\text{-body}) \quad n = \text{SCF, 2, 3, 4, ...} \quad (2)$$

where $n$ denotes the order of the MP theory. The analysis of the contents of the two- and three-body terms can be accomplished by connecting the supermolecular approach with the symmetry-adapted perturbation theory (SAPT).[2,3] The contents of $\Delta E^{(n)}$(2-body) are listed in Table 1. The SAPT energy corrections (see Table 1 and below) are denoted by $\epsilon^{(ij)}$, where $i$ and $j$ refer to the order of the intermolecular interaction operator and the intramolecular correlation operator, respectively.[2,3]

At the SCF level the interaction energy is divided into two parts: the Heitler−London (HL) interaction energy, which results from the unperturbed (but antisymmetrized) monomer wave functions, and the SCF-deformation energy, which describes the mutual polarization of monomers under the constraint of the Pauli principle. The former can be further divided into the electrostatic ($\epsilon_{es}^{(10)}$) and exchange ($\epsilon_{exch}^{HL}$) SAPT terms. This decomposition is similar in spirit to the partitioning of the SCF interaction energy pioneered some 30 years ago by Morokuma.[20]

In the second order of the MP perturbation theory the following terms appear: the second-order intrasystem correlation correction to electrostatics, $\epsilon_{es,r}^{(12)}$, the second-order dispersion term ($\epsilon_{disp}^{(20)}$), as well as exchange-correlation ($\epsilon_{exch}^{(2)}$) and deformation-correlation ($\Delta E_{def}^{(2)}$) terms. Only the first two are explicitly evaluated. More details about this partitioning can be found in ref 2.

The contents of the three-body interaction energies are obtained by eliminating all the additive terms. The latter include electrostatic energies at any order of the MP theory, $\epsilon_{es,r}^{(ln)}$, and dispersion energies of the second order with respect to the interaction potential, $\epsilon_{disp}^{(2j)}$. The nonadditivities which appear in the first three orders of the MP theory are listed in Table 1. More details about the partitioning of the three-body terms and their interpretation can be found in refs 2 and 21.

## B. Highly Correlated Treatments

The evidence gathered thus far is clear: to accurately reproduce the rotation−vibration spectra

and differential scattering cross sections, the potential-energy surface (PES) should be calculated at the coupled cluster with single, double, and perturbative triple excitations (CCSD(T)) level of theory. Of course, in many cases one can obtain valuable insights at the MP4 level (cf., e.g., Ar−OH[22]) or even MP2 level of theory (cf., e.g., the water dimer[23] or the HF dimer[24]), but in general, MP perturbation theory must be considered as divergent[25] and one should monitor its performance at critical points (minima and barriers) by means of CCSD(T). In particular, the MP approach may behave erratically upon monomer stretching[26,27] (see below for more discussion). Recently, it was found that UMP4 qualitatively failed to predict the shapes of the two PESs describing the interaction He−NO.[28] One may also anticipate particular cases where even the CCSD(T) level may not be sufficient. For instance, it has been recently argued that in the case of the CO dimer the correlation diagrams which occur only in the CCSDTQ approach may be needed.[29]

Complementary to the supermolecular approach is the SAPT formalism.[3,30] It attempts to reproduce all high correlation effects within a perturbation theory of intermolecular forces. SAPT offers well-defined and directly computable corrections of meaningful, intuitive interpretation. It allows the building of a hierarchy of model potentials which can produce accurate interaction energies if applied at the highest correlated level.

However, the power of SAPT—the perturbation expansion—is also its weakness. There are three convergence problems involved in SAPT: those with respect to the interaction operator, the intramonomer correlation operator, and symmetry forcing. For all many-electron problems the procedure is expected to be divergent.[31] Therefore, one should carefully monitor SAPT results with supermolecular calculations. In addition, the most accurate SAPT calculations practically always include the supermolecular SCF component[3,32] potential to avoid the prohibitive SAPT expansion of the induction energy.[33] Some difficult correlation terms in many-body interactions that are related to the induction effect are also often evaluated within the supermolecular approach.[34,35]

In conclusion, the supermolecular and perturbation approaches are in general complementary rather than competitive in calculating and modeling accurate PESs.

## C. New Developments

### 1. Density Functional Theory

The numerical results reported in numerous papers (cf. the recent review of Guo et al.[36]) suggest that density functional theory (DFT) yields reliable predictions of the geometries corresponding to the global minima on the PES and reasonable stabilization energies of some hydrogen-bonded and ionic complexes. In a recent study of the water dimer, it was shown that a full PES may also be obtained by means of a hybrid functional, adjusted to reproduce the experimental geometries of monomers and the dimer.[37] In general, however, the accuracy of reproducing the anisotropy of PESs was not tested carefully enough.

The suitability of DFT to deal with the intermolecular interactions is related to its ability to correctly account for all fundamental interaction components. However, it has been known for over two decades that unless nonlocal terms are included in the formalism, DFT is not able to reproduce the dispersion interaction.[38] Thus far, none of the existing variants satisfactorily meets this requirement.

This point has been recently demonstrated in calculations for several model systems: $OH^--H_2O$, $(H_2O)_2$, $CO-H_2O$, and $He-CO_2$.[39] An analysis of the results obtained using the B3PW91 functional in terms of SAPT suggested that this functional approximately reproduces electrostatic, induction, and exchange−induction energies at the correlated level of theory for electrostatically bound complexes ($OH^-H_2O$, $(H_2O)_2$) but no dispersion. For dispersion-bound complexes ($CO-H_2O$, $He-CO_2$), not only was the dispersion contribution missing, but also the electrostatic, exchange, and induction terms proved to be incorrect. Next, for strongly bound ionic hydrogen-bonded complexes, such as $OH^-H_2O$, the hybrid approach may indeed provide a reliable PES. For other systems, including water dimer, all tested functionals failed to reproduce the correct angular dependence, although the B3LYP and B3P86 functionals performed reasonably well for the most attractive geometries of the water dimer and $CO-H_2O$.

For now, DFT seems to have the potential for important achievements in the field of molecular interaction, especially for large systems, but we must overcome the dispersion problem and achieve better control over its accuracy. The first promising attempts to combine DFT and the long-range dispersion component presented by Gianturco and collaborators[40] should be mentioned in this context.

### 2. Local-Correlation Methods

The local-correlation method[41,42] has recently emerged as an alternative supermolecular approach for the study of intermolecular interactions.[43,44] Although the primary goal of local-correlation methods has been to reduce the steep dependence of the computational cost on the size of the chemical system, they also introduce some conceptual advantages for studying intermolecular interactions, such as reduced BSSE,[43] and the possibility of decomposing the local-correlation energies into different excitation classes.[44] In particular, it was shown that the LMP2 and CP-corrected MP2 equilibrium properties for the water dimer,[43] water clusters,[44] and model dimers of gold[45] are fairly close. One may expect that LMP2 will become an important ab initio alternative or a complementary approach to DFT. As noted in the previous section, the state of the art DFT misses some important interaction terms, in particular the dispersion contribution. In contrast, LMP2 derives the interaction energy at the MP2 level of theory, which correctly includes all fundamental components of the interaction energy, including the dispersion term.[2,46] The LMP2 interaction energies may be

directly verified by the SAPT treatment, as well as supermolecular higher-order MP or CC calculations. In addition, the localized treatment is currently being extended to the higher levels of the MP (LMP4(SDQ)[47]) and CC (LCCSD[48]) theories.

## D. Basis-Set Issue

### 1. Basis-Set Superposition Error

Basis-set superposition error (BSSE) may be viewed as a special and separate basis-set problem. For a long time progress in ab initio calculations of intermolecular forces had been strongly hindered by BSSE. Introducing the CP correction for BSSE[15,16] proved to be crucial to the present success of the supermolecular approach to the van der Waals complexes.[2,4] Whereas occasionally one may obtain better numbers by keeping BSSE as a counterbalance for the basis-set unsaturation, such a policy should be discouraged and, as aptly summarized by Taylor,[49] "relying on such cancellation to occur in a wide range of situations seems to be ludicrously optimistic". Since radial and angular dependence of BSSE is different from that of the interaction energy, it may result in PESs with unphysical characteristics. Consequently, even gradient optimization should be performed with a proper account of BSSE as demonstrated by Simons et al.[18] and Hobza et al.[19]

Somehow, the argument of the overcompensation by the CP lingers in the literature,[50] despite many formal and numerical proofs to the contrary.[23,51−57] More new numerical arguments in favor of the CP correction appeared recently in the work of Halkier et al.,[23] who demonstrated that only the CP-corrected interaction energy behaves as a well-defined correlation portion of the interaction energy, reinforcing the findings of refs 51−57. Another strong and novel argument that overcompensation does not take place resulted from a comparison with (almost) BSSE-free formalisms, such as Meyer's chemical Hamiltonian approach (CHA)[51,58] or the local-correlation method.[43,45] In particular, the recent study of Mayer and Valiron revealed an excellent agreement of the MP2−CHA BSSE-free interaction energies and the MP2−CP-corrected results.[58] The local-correlation method also brings the interaction energy into much closer agreement with the counterpoised result.[43,45]

The problem with CP is that its usefulness is restricted to the van der Waals region, where the monomers are distinguishable and their distortions do not approach the bond-breaking point. For a reactive PES, these conditions are no longer satisfied. Suppose we study a reaction

$$A + D \rightarrow A{-}D \rightarrow [X]^{\ddagger} \rightarrow B{-}C \rightarrow B + C$$

which involves reactants A and D, their van der Waals complex A−D, a transition-state complex X, the van der Waals complex B−C, and products B and C. Ideally, one would like to have a basis-set consistent evaluation of every step of this process, i.e., at each point of the complete PES for the reaction. Yet, there is one CP correction for the reactant complex, another for the products, and no recipe at all to define this correction for the transition state. There is no noticeable progress in dealing with this problem.

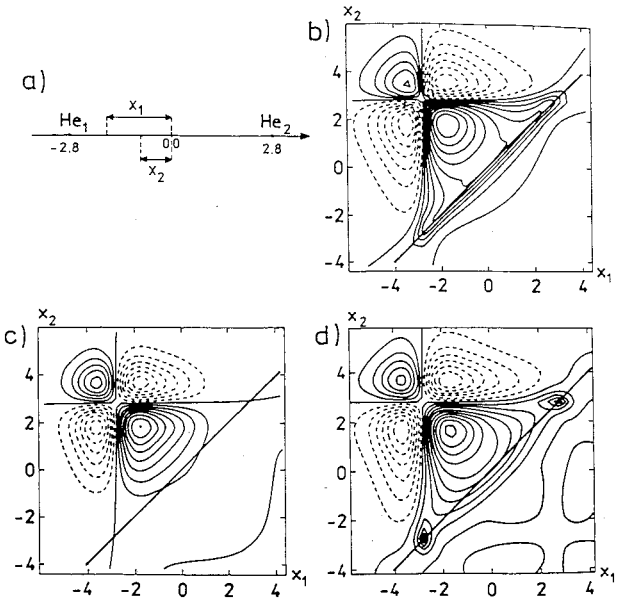


**Figure 1.** Plots of the dispersion function for the equilibrium He dimer from ref 61. The electron coordinates, $x_1$ and $x_2$ are defined in part a. The accurate dispersion function (calculated with Gaussian geminals) is shown in plot b. If the dispersion term is calculated with a monomer-centered basis set, one obtains plot c. If every electron is allowed to use the complete dimer-centered basis set (DCBS) as well as the bond functions, one obtains plot d.

In van der Waals complexes involving an open-shell moiety, which are often described by multiple PESs, the treatment of BSSE is more involved. The issues associated with this treatment will be discussed in section III.C.3.

### 2. Basis-Set Saturation

Basis-set saturation at the correlated level, despite some progress, still poses a problem. It originates in the Coulomb cusp condition which is very slowly reproduced by one-electron basis-set expansion.[59,60] It demands very high polarization functions—so high that the largest of the correlation-consistent sets, d-aug-cc-pV6Z, is still not good enough.[23] In van der Waals complexes, this effect is particularly serious for the dispersion interaction—the intermolecular correlation effect. The situation is visualized in Figure 1 (see ref 61). The "exact" dispersion fragment of the wave function has a vertical "cliff" in the cusp region (Figure 1b), whereas a finite one-electron basis-set expansion is able to produce only a mild slope in this region (Figure 1c).

At present, there are essentially two ways of alleviating the problem. A rigorous solution consists of using a basis set that includes the interelectron distance $r_{12}$ explicitly. In this context, the explicitly correlated Gaussian geminals offer the most accurate approach,[62−64] although so far the huge number of nontransferable nonlinear parameters renders the method extremely difficult in actual applications, e.g., to $H_2O$[63] and to $He_2$.[64,65] A viable alternative is offered by the R12 method.[59,60] This method includes terms in the wave function that are linear in $r_{12}$. The latter

**Table 2. Well Depth, $D_e$, for $Ar_2$ Obtained by CCSD(T) with Basis Sets with and without Bond Functions (energies in $cm^{-1}$)[a]**

| basis set | $D_e$ | basis set + bf | $D_e$ |
|---|---|---|---|
| aug-cc-pVDZ | 26 [70] | | |
| d-aug-cc-pVDZ | 33 [70] | | |
| aug-cc-pVTZ | 67 [70] | aug-cc-pvtz + bf(332) | 92 [70] |
| | | aug-cc-pvtz + bf(33211) | 97 [70] |
| d-aug-cc-pVTZ | 81 [70] | | |
| aug-cc-pVQZ | 82 [70] | aug-cc-pvqz + bf(332) | 96 [71] |
| d-aug-cc-pV6Z | 96 [72a] | | |
| exp | 99 [72b] | | |

[a] All values are counterpoise-corrected. The bond function symbol bf(332) represents (3s,3p,2d) and bf(33211) represents (3s,3p,2d,1f,1g) bond functions.

approach proved to be very efficient for $He_2$,[66] several hydrogen-bonded dimers,[23] water trimer,[67] and HF oligomers.[68]

A simpler approach, although not so accurate and rigorous, involves the use of bond functions located in the middle of the van der Waals bond.[61,69,70] One can see in Figure 1d that the dispersion function, which includes bond functions, performs much better in the cusp region and the "cliff" of the cusp area is reproduced much more accurately. Indeed, recovering the cusp in terms of the multicenter expansion is significantly more effective. The efficiency of the bond functions in reproducing the values of the interaction energy is demonstrated in Table 2.[70,71]

One can see that the d-aug-cc-pV6Z result for $D_e$ can be reproduced with a much smaller aug-cc-pVTZ + bf(33211). At the same time, the pure aug-cc-pVTZ basis set yields only 60% of $D_e$. We also note that the best ab initio result obtained with d-aug-cc-pV6Z is still 2−3% off the empirical value. This slow convergence of the correlation-consistent hierarchy of basis sets accompanied by a rapid increase of the number of functions was commented on by the van Duijneveldts as "somewhat alarming"[73] and justifies parallel work on customized and specialized selections as the medium-sized polarized basis sets appropriate for molecular properties and interactions[74] or an extended and refined basis for a water dimer.[75]

The above results are representative for dispersion-bound complexes. One has to keep in mind that bond functions cure the problem of the intermonomer-correlation cusp but are not appropriate for intramonomer-correlation effects and electric monomer properties.[61] It is thus possible that the latter quantities are distorted and the anisotropy of electrostatic interaction modified in an artificial manner. A more detailed discussion of this problem was reported in ref 61.

## E. State of the Art Example

Most ab initio calculations of van der Waals complexes attempt to characterize the geometry, energetics, and local curvature in the minimum. A number of benchmark calculations of the equilibrium van der Waals distance ($R_e$), well-depth ($D_e$), and other characteristics have recently been performed with a sequence of aug-cc-pVNZ basis sets[76] at the CCSD(T) level of theory. These include rare-gas dimers,[72a,77] rare-gas−molecule complexes (Ar−$H_2$,[78] Ar−HF,[79] Ar−HCl[78]), and hydrogen-bonded dimers.[80] The $R_e$ and $D_e$ parameters have been estimated with close to spectroscopic accuracy, but it should be noted that the necessity of including the "complete basis set" (CBS) extrapolations,[77] even with the largest aug-cc-pV5Z basis set, is disturbing.

However, the $R_e$ and $D_e$ parameters and description of other stationary points do not tell the whole story about the complex. The goal for such floppy, anharmonic systems should be the accurate characterization and analytical representation of the global potential-energy surface. Together with multidimensional quantum treatments of the nuclear dynamics, this allows for a quantitative comparison with the spectroscopic data. In this context, complexes of rare gases with a variety of molecules provide especially useful model systems. On the one hand, a highly resolved rotation−vibration spectra, for ground and excited states, may be measured and assigned for these systems. On the other hand, the intermolecular PES has few dimensions and may be fitted exactly. Furthermore, the quantum treatment of nuclear dynamics in this case is relatively simple and may be performed with accuracy far greater than the accuracy of the electronic structure calculations. Comparison of ab initio and experimental frequencies thus yields a very stringent test of the ab initio PES. Such a test may be extended to other measurable properties of the system. These include primarily rotationally inelastic scattering cross sections but also such macroscopic properties as virial, viscosity, diffusion, and thermal diffusion coefficients.

How accurately are we able to reproduce spectroscopic and other properties by the state of the art ab initio calculations? We will illustrate this by a recent, very thorough study of the Ne−CO complex.[81,82] Two very highly accurate PESs have been obtained: one from supermolecular CCSD(T) calculations[81] and another from SAPT.[83] The differences between these two PES are essentially small: the potential well on the CCSD(T) PES is slightly shallower and less anisotropic than that on the SAPT surface. The low-energy repulsive wall on the CCSD(T) surface is also less anisotropic than that of the SAPT surface.

As shown in ref 81, both surfaces perform very well for a variety of properties of the Ne−CO complex. Rotation and rotation−vibration spectra are reproduced with spectroscopic accuracy, well below 1 $cm^{-1}$. The microwave absorption spectra, for rotational transitions ranging from $1_{01}-0_{00}$ to $4_{14}-3_{13}$, are reproduced with errors: 0.008 (SAPT), 0.016 $cm^{-1}$ (CCSD(T)). The infrared spectra are also in excellent agreement: For the ground state, for $J = 1-7$, $K = 1-3$, the error ranges from 0.070 to 0.330 $cm^{-1}$ (SAPT) and from 0.250 to 0.500 $cm^{-1}$ (CCSD(T)). For the first excited bending state, for $J = 0-7$, $K = 0-1$, the error ranges from 0.200 to 0.670 $cm^{-1}$ (SAPT) and from 0.05 to 0.260 $cm^{-1}$ (CCSD(T)). The experimental, CCSD(T) and SAPT fundamental bending frequencies are 8.5805, 8.359, and 8.253 $cm^{-1}$, respectively. Both potentials perform remarkably well, SAPT giving somewhat better results for the ground state whereas CCSD(T) giving better ones for the excited state.

Another stringent test of the potentials is provided by the state-to-state cross sections for rotational excitation of CO by Ne. The integral cross sections have been measured and compared to those calculated with the SAPT and CCSD(T) potentials. Both surfaces predict more scattering into high rotational levels than is observed. The feature of the integral cross sections most sensitive to the potential surface is the interference structure that appears at low $\Delta j$. The CCSD(T) surface predicts the phase interference oscillations correctly, although it does not reproduce the amplitudes particularly well. The SAPT surface predicts the wrong phase at low $\Delta j$. It thus appears that the CCSD(T) surface is more accurate in the repulsive region. State-to-state differential cross sections would provide a much more exacting test since the rainbow maxima and minima of SAPT and CCSD(T) are distinctively shifted with respect to each other.

An important property is pressure broadening. Both surfaces predict broadening cross sections well within the experimental error estimate (which are on the order of $\pm 10\%$) and very close to each other (within 1−2%).

The virial coefficients computed from the SAPT potential are lower than those computed from CCSD(T) at all temperatures. The consistent difference reflects the deeper well and slightly smaller repulsive core of the SAPT potential. The two potentials' predictions are all within the experimental error bars. Experimental accuracy on the order of 1 $cm^3$/mol, not achievable with the best current techniques, would be required to cleanly select one of the two potentials over the other.

Concluding the above comparisons, both potentials certainly achieve spectroscopic accuracy (less than 1 $cm^{-1}$ error). SAPT gives a slightly better description of the ground state and of the well region since it is somewhat deeper. CCSD(T) gives a better description of excited vibrational states and rotational excitation cross sections since it has a more realistic shape in the repulsive wall.

The errors in the CCSD(T) and SAPT potentials have two origins: finite basis-set size and incomplete treatment of electron correlation. The more serious of the two is the basis-set effect. In addition, SAPT is affected by the approximate evaluation of the exchange effects, which becomes serious for the repulsive wall. The fact that SAPT performs better in the well region but worse in the repulsive region seems to be related to the cancellation of the basis-set effect and exchange effect. An additional source of errors in both cases may be due to the neglect of the intramonomer stretch in the vibration dynamics calculations (see section III.A.1 for more discussion).

The above results are representative of what can be achieved today. For specific systems, e.g., complexes with helium (He−HF[84] and He−CO[85]), one can achieve even greater accuracy. In general, spectroscopic accuracy may be occasionally reached for systems as large as Ar−benzene.[86] The highly accurate potentials may be further scaled or adjusted to provide hybrid potentials with even greater accuracy.[87]

## III. Challenges

### A. Inclusion of Intramolecular Degrees of Freedom

Most of the PESs which are currently available involve the interacting molecules treated as rigid bodies in their equilibrium or vibrationally averaged geometries. Such an approach provides a PES which depends only on the intermolecular degrees of freedom. This is a reasonable approximation which allows us to predict, e.g., the intermolecular vibration−rotation−tunneling (VRT) dynamics[88] and other properties discussed above. However, a number of important phenomena, such as intramolecular frequency shifts, vibration predissociation, intramolecular vibrational redistribution, etc., cannot be studied with such potential functions. There is an urgent need for PESs with intramolecular-coordinate dependence, especially for heavy-atom rotors where the small line spacing poses problems to inversion of spectroscopic data. Therefore, one of the serious challenges to ab initio treatment is to provide insights into the construction of fully dimensional PESs, which would include both inter- and intramolecular degrees of freedom. The task of building such surfaces becomes progressively more complex as the number of atoms increases.

#### 1. Atom–Linear Molecule Case

In atom−diatom clusters, the development of full three-dimensional PESs was pioneered by LeRoy and Hutson.[89] Due to the fact that for atom−diatom systems the rotation−vibration energy levels can be calculated exactly, the high-resolution spectroscopic data have been used to fit a number of benchmark PESs. The functional form of these PES generally involves expressions (in Jacobi coordinates) of the type

$$V(R,\Theta,r) = V_{sh}(R,\Theta,r) + V_{lr}(R,\Theta,r) \qquad (3)$$

where $r$ represents the intramonomer bond distance in a diatomic molecule and $V_{sh}$ and $V_{lr}$ denote short-range and long-range potential-energy terms. In practice, however, the explicit $r$-dependence is avoided by applying a quasi-Born−Oppenheimer approximation to separate "slow" and "fast" vibrational modes. Such a procedure replaces the $r$-dependence by a manifold of $V(R,\Theta)$ surfaces for different values of the intramolecular vibrational quantum number $v$[90] (see below). This form of the potential allows one to study vibrational frequency shifts.

From the ab initio standpoint, the construction of intramolecular coordinate-dependent PESs should take into consideration two effects: the monomer deformation energy and the change in the two-body interaction energy terms caused by deforming a monomer (cf. eq 1). The first is the so-called one-body term, and its computational requirements are well-known. A less obvious problem is how to describe the variation of two-body terms as a function of intramolecular geometry.

The theoretical and computational aspects of this dependence were analyzed by Rak et al. for a model

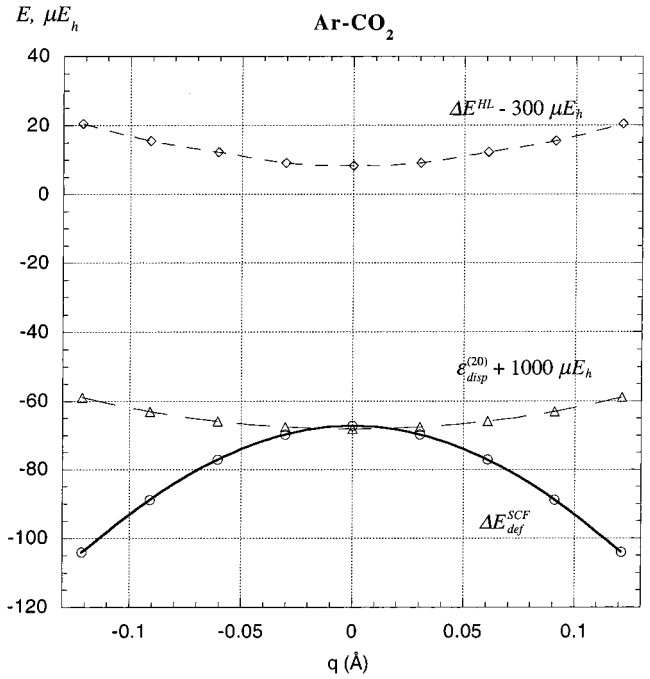


**Figure 2.** Dependence of the interaction energy components of Ar−$CO_2$ complex upon the asymmetric stretching coordinate $\vec{q}_3 = 0.33\vec{x}_1 - 0.88\vec{x}_2 + 0.33\vec{x}_3$, where $\vec{x}_i$ refers to unit vector displacements from equilibrium of O, C, and O, respectively (in $\mu E_h$).[27]

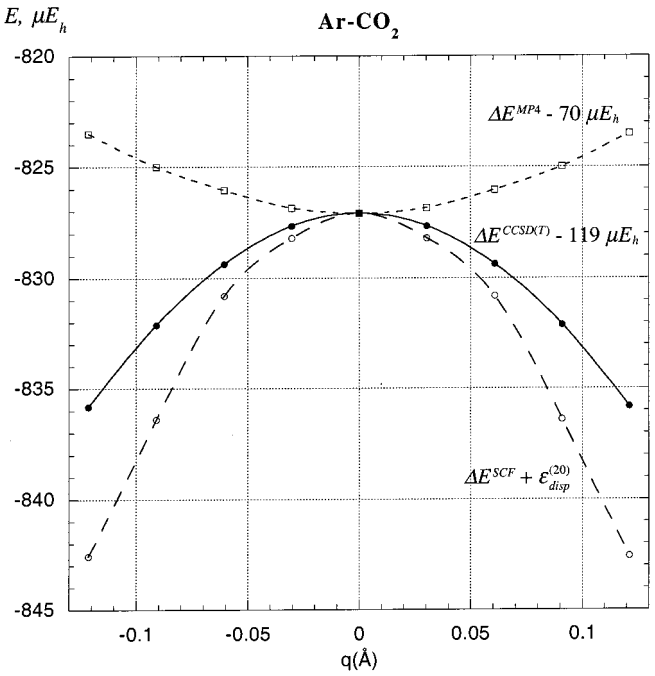


**Figure 3.** Dependence of the correlation components of Ar−$CO_2$ complex upon the asymmetric stretching coordinate $\vec{q}_3 = 0.33\vec{x}_1 - 0.88\vec{x}_2 + 0.33\vec{x}_3$, where $\vec{x}_i$ refers to unit vector displacements from equilibrium of O, C, and O, respectively (in $\mu E_h$).[27]

system, Ar−$CO_2$. This complex has the equilibrium T-shaped geometry with the intersystem Ar−C distance of 3.704 Å.[27] At the equilibrium distance $R$, the interaction energy terms were calculated as functions of the displacements of the atoms of $CO_2$ along the asymmetric stretching coordinate of $CO_2$, $q_3$. The results are presented in Figures 2 and 3.

The plot of $\Delta E^{HL}(q_3)$ shows that this term becomes more repulsive as the molecule becomes distorted, indicating that the overlap increases along the $q_3$ coordinate. The shape of electron density around $CO_2$, revealed via a plot of the Laplacian of electron density ($-\Delta\rho$),[91] indicates a depletion of density around the C atom and concentrations around the O atoms. When $CO_2$ is distorted along the normal mode $q_3$, the depletion travels along with the C atom. The Ar atom thus faces the region of higher density which results in larger HL repulsion.

The induction effect, described by $\Delta E_{def}^{SCF}(q_3)$, leads to a stronger stabilization as the molecule becomes distorted. It can be easily rationalized using the multipole expansion of induction energy. If $CO_2$ is not deformed, the first nonvanishing induction term varies as $R^{-8}$. A deformed $CO_2$ acquires a dipole moment, which gives rise to induction terms proportional to $R^{-6}$.

The dependence of correlated terms upon $q_3$ is even more interesting (Figure 3). The second-order dispersion energy $\epsilon_{disp}^{(20)}(q_3)$ shows an upward trend with $q_3$. However, when $\epsilon_{disp}^{(20)}$ is combined with the SCF interaction, the total effect follows the behavior of the SCF energy and varies downward. The MP4 and CCSD(T) interaction energies display *opposite* behaviors with respect to $q_3$. Only CCSD(T), however, is consistent with the experimentally observed red shift of the asymmetric stretching frequency. The failure of MP4, an otherwise fairly well correlated level of theory, results from a worsening convergence of the Møller−Plesset perturbation theory as the C=O bonds become distorted, which results in the wrong curvature of the PES. The CCSD(T) approach seems to behave correctly upon the C=O stretch.

In the benchmark complex Ar−HF, the dependence of the Ar−HF potential on HF stretching coordinate, $r$, was studied by Chuang et al. at the CCSD(T) level of theory.[92] They found that the dependence of the intermolecular potential on $r$ is very anisotropic, being maximal for $\Theta = 0°$, and becoming essentially independent of $r$ at $\Theta > 45°$.

For the same complex, the full dimensional $V(R,\Theta,r)$ PES evaluated by SAPT was used by Jeziorska et al.[93] to investigate the effects of HF rigidity on the rovibrational spectrum by comparing the spectra calculated using the three-dimensional PES and its reduced-dimensionality variants. The best results were obtained when the three-dimensional PES was averaged over the monomer vibrational states as $\langle V\rangle_v = \langle\chi_v|V(R,\Theta,r)|\chi_v\rangle$, where $\chi_v$ represent the vibrational wave functions of HF (see ref 94). Such effective potentials were shown to reproduce the rovibrational states of this complex with the accuracy of 0.1 $cm^{-1}$ compared with the full three-dimensional calculations. However, they also demonstrated that the two-dimensional PESs evaluated in rigid-monomer approximation lead to much less reliable predictions. In particular, the $V_v(\Theta,R) = V(\Theta,R,\langle r\rangle_v)$ two-dimensional PESs, evaluated at $r = \langle r\rangle_v$, i.e., the average anharmonic values of $r$, were shown to be unsuitable for the calculations of red shifts in this complex.

The form of PES as described by eq 3 is inappropriate for atom−diatom interactions when the intramolecular coordinate $r$ is stretched to the point

of dissociation. In such circumstances an atom−atom potential representation may be advantageous. Such a representation has been particularly popular for representing the interactions between rare gases (RG) and halogen molecules $X_2$

$$V_{RG-X_2}(R,\Theta) = V_{RG-X}(\rho_a,\gamma_a) + V_{RG-X}(\rho_b,\gamma_b) \quad (4)$$

where $\rho_a$, $\rho_b$ and $\gamma_a$, $\gamma_b$ are polar coordinates (radii and angles, respectively) describing a position of RG with respect to two halogen atoms a and b (see ref 95). The atom−atom potentials are described as

$$V_{RG-X}(\rho,\gamma) = V_\Sigma(\rho)\cos^2\gamma + V_\Pi(\rho)\sin^2\gamma \quad (5)$$

where $V_\Sigma$ represents the $^2\Sigma$ state of the RG−X interaction while $V_\Pi$ represents the $^2\Pi$ state.[95] This diabatic representation is particularly useful when eqs 4 and 5 are used to fit the ab initio points. For example, Williams at al.[96] used this form to fit the PES of $He(^1S) + Cl_2(B^3\Pi_u)$ interaction energy points evaluated at different Cl−Cl interatomic distances. In the asymptotic Cl−Cl dissociation limit, these authors used the ab initio derived $^2\Sigma$ and $^2\Pi$ potential of He−Cl. Naumkin and McCourt used the potential form eqs 4 and 5 to fit ground-state surfaces for He−$Cl_2$[97] and Ar−$Cl_2$.[98]

In a study involving a simulation of the ($B$, $v' = 8,10,12$, $j$) ← (X,$v'' = 0$,$j$) excitation spectrum of the $HeCl_2$ complex, the full dependence of the final PES upon the intramolecular stretching coordinate was included.[26,96] The final state in this process is the PES representing the interaction between the excited triplet state of $Cl_2$ interacting with He, i.e., the PES of $He(^1S) + Cl_2(B^3\Pi_u)$, with highly excited vibrational $Cl_2$ states. The interaction with He lowers the Π symmetry of $Cl_2$ to A′ and A″, depending on the orientation of the singly occupied $\pi^*$ orbital of $Cl_2$ with respect to the triatomic plane. The A′ and A″ PESs were evaluated[26,96] at two levels of theory, UMP4 and UCCSD(T), at different Cl−Cl distances. The $^3$A′ PES evaluated at the UMP4 level showed clear symptoms of a breakdown, especially at stretched Cl−Cl distances. UCCSD(T) raised this surface by nearly 30% while leaving the A″ surface essentially unaffected.

Both studies outlined here emphasize that the MP4 level of theory is inadequate in the calculations of PESs which include the dependence of the intramolecular stretching coordinate. Such PESs should be derived at the UCCSD(T) or at a multireference level of theory. The single-reference UCCSD(T) approach, which is known for its correct asymptotic behavior upon dissociation,[99] provides the most efficient remedy. Single reference RCCSD(T) is known to be less robust for large stretches.[99]

In some instances the atom−molecule PES may constitute a part of a larger reactive surface. For example, in the reactions $X + H_2 \rightarrow HX + H$ (X = F, Cl) the entrance valley was shown to contain a van der Waals well related to an intermolecular T-shaped complex $X-H_2$(X = F, Cl). Although this long-range complex can be represented by the PES of eqs 3 and 4, it is more convenient to represent the entire reactive surface using a many-body expansion

$$V = \Sigma V_{1-body} + \Sigma V_{2-body} + V_{3-body} \quad (6)$$

where 1-body, 2-body, and 3-body represent, respectively, atomic, atom−atom, and atom−atom−atom terms. Such a form is better suited for a bond breaking/formation in the course of a reaction. Werner and co-workers used this potential form to fit the $F + H_2$ [100] and $Cl + H_2$ [101] reactive surfaces.

### 2. Diatom–Diatom Case

To date, the diatom−diatom analytical ab initio-based PES, which include both intra- and intermolecular degrees of freedom (i.e., six-dimensional PESs), exist only for dimers of hydrogen halides $(HF)_2$ and $(HCl)_2$. However, in neither case could the PESs be considered as purely ab initio. The surfaces for $(HF)_2$ were advanced by Quack, Suhm, and collaborators.[24,102] The form of PES for $(HCl)_2$ was initially proposed by Bunker et al.[103] and fitted to the ab initio points of ref 104.

$(HF)_2$ is one of the simplest hydrogen-bonded dimers, but assembling the full-dimensional PES required a great deal of effort. The analytical form of this potential, though extremely complex, was based on multipole-expanded long-range terms and Morse functions to describe the intramonomer stretching coordinates. Elaborate couplings between inter- and intramolecular degrees of freedom were also included. The earlier version, SQSBDE, was fitted to the average coupled pair functional (ACPF) calculations and adjusted to rovibrational spectra and to the value of the dissociation energy $D_o$.[102] The newest versions, SO-3 and SC-2.9, were fitted to the grid of over 3000 MP2−R12 points and empirically adjusted as well.[24] The six-dimensional vibrational calculations on the SQSBDE surface were carried out by Wu et al.[105] and Zhang et al.,[106] and the preliminary analysis of the vibrational dynamics on the new surfaces was carried out by Klopper et al.[24]

For $(HCl)_2$, the ab initio six-dimensional PES of Bunker et al.[103] was fitted to the ab initio ACPF data. The pure ab initio surface was not accurate enough to reproduce the spectral features of this complex. To improve the intermolecular region, Elrod and Saykally empirically adjusted the surface by a direct nonlinear least-squares fit to the available microwave, far-IR, and near-IR data.[107] The detailed analysis of the vibration dynamics on the adjusted PES, dubbed ES1, was carried out by Qiu and Bačič, who carried out exact bound-state calculations of the rovibrational levels of this complex.[108]

The availability of the full-dimensional $(HF)_2$ and $(HCl)_2$ PESs offers a unique opportunity to assess the validity of rigid-monomer approximation in the context of molecule−molecule interactions. On the basis of both six- and four-dimensional calculations for $(HF)_2$, Zhang et al.[106] concluded that the fixed-monomer approximation has very little effect on $D_o$ (ca. 6.6 $cm^{-1}$) and on the intermolecular rovibrational levels (with differences not exceeding 2 $cm^{-1}$). The ground-state donor−acceptor interchange tunneling splitting was also very similar in the four- and six-dimensional approaches (0.48 vs 0.44 $cm^{-1}$, respectively). They concluded that the coupling between the

intra- and the intermolecular vibrations in $(HF)_2$ is weak.

Similar conclusions were initially drawn for $(HCl)_2$ by Qiu and Bacič.[108] $D_o$ was underestimated by only 5.5 $cm^{-1}$, and the intermolecular rovibrational levels differed very little (less than 2 $cm^{-1}$) by assuming the rigid-monomer approximation. The predictions of the ground-state tunneling splitting by the four- and six-dimensional approaches were also very close (15.48 vs 14.94 $cm^{-1}$, respectively). These results indicated that on the ES1 surface the coupling between the inter- and intramolecular degrees of freedom was very weak. However, the study of the tunneling splitting between vibrationally excited monomers by Qiu et al.[109] revealed a serious flaw of that surface.

The donor−acceptor interchange tunneling when one of the monomers is vibrationally excited serves as a keen measure of the inter−intra couplings because in this process the changing role of the donor and acceptor is accompanied by the transfer of a intramolecular vibration quantum from one monomer to the other. Qiu et al.[109] found that the ES1 surface failed by showing this splitting to be nearly zero, in contrast to experimental findings. In their judgment, the flaws of the ES1 surface stem from the inability of the ACPF calculations, to which the surface was fitted, to correctly account for the coupling between the inter− and intra−intermolecular degrees of freedom in this system. These couplings require a highly correlated ab initio treatment (cf. section III.A.1), certainly higher than that of ACPF. To summarize these important findings in the authors own words, "the accurate description of the ground-state splitting in itself does not guarantee that the PES will perform with the comparable success in case of tunneling when one of the monomers is vibrationally excited".[109]

Interestingly, the excited-state splitting was reasonably well reproduced in $(HF)_2$ on the SQSBDE surface according to Zhang et al.[106] The analogous calculations on the new SO-3 and SC-2.9 surfaces for $(HF)_2$ have not been published yet (see ref 24).

### 3. Polyatomic Trimer Case

It is highly unlikely that potential-energy surfaces of the same complexity as those for $(HF)_2$ and $(HCl)_2$ can be developed for larger polyatomic dimers and trimers at this time. For the water trimer, only rigid analytical potentials are available.[110,111] However, formation of clusters of water has a dramatic effect on the structural and vibrational properties related to the intramolecular degrees of freedom. For example, the equilibrium O−H bond length in the isolated $H_2O$ molecule is 0.9572 Å, while the same distance in the antiferroelectric ice Ih is 0.99 Å. For these reasons, Rak et al.[13] examined to what degree the rigidity of the O−H bonds affects the three-body terms in $(H_2O)_3$. They considered a cyclic $C_1$ trimer configuration where the lengths of the proton-donor O−H bonds were stretched in a concerted fashion from the gas-phase value of 0.9572 Å to the value 0.99 Å. The dependence of the three-body interaction energy terms is shown in Figure 4. In the range of

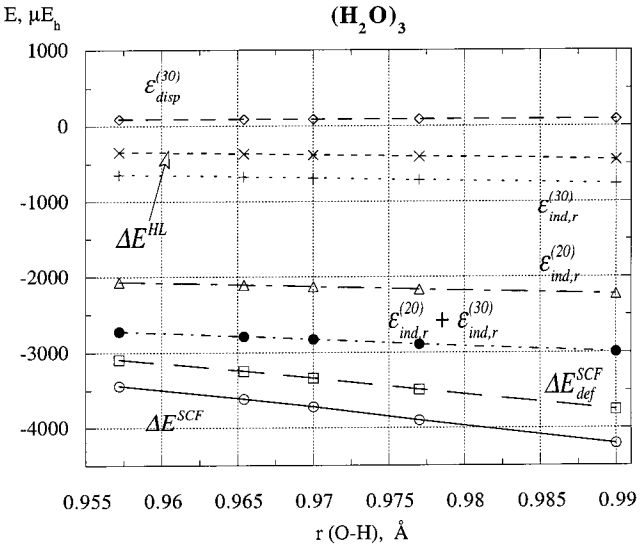


**Figure 4.** Dependence of three-body interaction energy components of cyclic $C_1$ water trimer upon the concerted stretch of the hydrogen-bonded O−H bonds.[13]

O−H variations considered, the three-body energy components vary linearly with respect to the O−H stretch. This fact contrasts water from $Ar_2CO_2$ (see below), where the dependence upon the stretch was strongly nonlinear. Both the dispersion and HL-exchange nonadditivities are very small and vary negligibly with $r$(O−H). The $\Delta E_{def}^{SCF}$ nonadditivity, on the other hand, leads to some 700 $\mu E_h$ gain in stability while the O−H bonds are stretched from 0.9572 to 0.99 Å. It should be emphasized that this additional stabilization remains neglected by the polarized water models which employ rigid monomers, such as the PES of Millot and Stone[110] or the SAPT surface.[111]

## B. Nonadditive Interactions

### 1. General Outline

The nonadditive components of the interaction energy in a trimer arising in different orders of the supermolecular and SAPT methods are listed in Table 1. One can see that besides the fundamental nonadditive terms, induction, dispersion, and exchange, a number of coupling terms appear, such as exchange−induction, induction−dispersion, or exchange−induction−dispersion, etc. If one performs highly correlated calculations, e.g., by the CCSD(T) method, all these contributions are implicitly recovered. When one also aims at an analytical modeling, the separation of different components is essential since they have different functional behavior. The recent advances in calculations of various contributions by SAPT have been described in refs 34, 35, and 112−114.

Three-body forces in trimers are commonly quite small, on the order of a few percent of the total interaction energy.[115,21] In larger clusters, however, their role rapidly increases reaching 10−30% and more.[116−118] For instance, in the $(HF)_n$ oligomers, two- and three-body terms are essential for a description of the hydrogen bond whereas four- and $n$-body contributions quickly decline with $n$.[68]

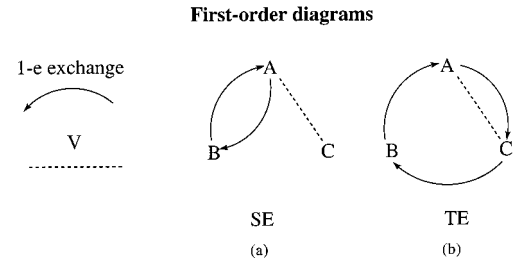


**Figure 5.** Diagrams representing the Heitler−London exchange terms: (a) single exchanges (SE) and (b) triple exchanges (TE). The electron exchange operators are symbolized with arrows and the interaction operator with a dashed line.

When choosing a computational procedure, it is very important to fully appreciate the complex nature of the three-body forces in a given cluster. For instance, in the water trimer the dominant three-body term originates from induction interaction and is almost completely recovered (along with the accompanying exchange effects) at the SCF level of theory.[119,120] Clusters involving polar molecules and cations are also dominated by the induction nonadditivity. Clusters including polar molecules and anions, on the other hand, are more complex as the diffuse electronic charge gives rise not only to the induction nonadditivity but also to exchange and dispersion, cf., e.g., $OH^-(H_2O)_n$.[117]

The largest contributions to the three-body term in nonpolar trimers (e.g., the methane trimer[121]) are from dispersion and exchange effects. It has been shown that the lowest level of theory to correctly account for both is MP3.[2,21] However, important intramonomer correlation corrections do not appear until the fifth order, MP5, or CCSD(T), as demonstrated for rare-gas trimers.[122]

Perhaps the most revealing case includes both polar and nonpolar species, such as rare gases bound to a chromophore. For there all fundamental and a number of coupling terms should be accounted for.[2,21,35,114,123,124] Again, MP3 is the lowest acceptable level of theory which accounts for the bulk of the three-body effects, but in order to include intramonomer correlation corrections, it is necessary to perform MP4 and CCSD(T) calculations or high-order SAPT calculations.

Below we will describe recent advances in the calculation and modeling of various nonadditive terms, with special emphasis on the exchange effects.

### *2. Evaluation of Single and Triple Exchange Terms: Pseudodimer Approach*

Jansen[125] first recognized two mechanisms of exchange effects with different asymptotic behavior (see also Cooper and Hutson[126]). These originate from terms involving exchange within a pair of monomers and among all three monomers, respectively. Terms which involve only a single exchange within a pair of monomers are called single-exchange (SE) terms (Figure 5a). Terms which involve exchange among three monomers are referred to as triple-exchange (TE) terms (Figure 5b)[35] (strictly speaking, these are *cyclic* single-exchange terms[113,127]). It should be stressed that the two exchange mechanisms appear in every order of SAPT.[35] However, their explicit calculation is relatively easy only in the first order.[127]

To separate these effects, a method of evaluating SE three-body exchange terms was developed.[35] It involves treating the trimer as a pseudodimer consisting of a dimer and a monomer

$$P_{\mathrm{corr}}(\mathrm{AB\cdots C}) = \epsilon_{\mathrm{corr}}(\mathrm{AB\cdots C}) - \epsilon_{\mathrm{corr}}(\mathrm{A\cdots C}) - \epsilon_{\mathrm{corr}}(\mathrm{B\cdots C}) \quad (7)$$

where $\epsilon_{\mathrm{corr}}$ refers to a particular perturbation correction derived for the pair in parentheses and $P_{\mathrm{corr}}$ represents the resulting nonadditive contribution. In particular, the electrostatic interaction within the pseudodimer AB···C is given by

$$P_{\mathrm{es}}^{(10)}(\mathrm{AB\cdots C}) = \epsilon_{\mathrm{es}}^{(10)}(\mathrm{AB\cdots C}) - \epsilon_{\mathrm{es}}^{(10)}(\mathrm{A\cdots C}) - \epsilon_{\mathrm{es}}^{(10)}(\mathrm{B\cdots C}) \quad (8)$$

Chałasiński et al.[35] showed that when the dimer AB is described by a Heitler−London wave function, $P_{\mathrm{es}}^{(10)}$(AB···C) describes the SE term, related to the exchange between A and B, with minor contributions from terms involving multiple exchanges between A and B. The SE contribution to the (AB···C) term is schematically represented by diagram a of Figure 5. To recover the whole SE term, contributions from the remaining pseudodimers must be added. $P_{\mathrm{es}}^{(10)}$(AB···C) describes the electrostatic interaction of multipoles on monomer C with multipoles due to exchange between A and B, and therefore, in the presence of a permanent multipole on C, $P_{\mathrm{es}}^{(10)}$(AB···C) decays as $R^{-n}$ with respect to AB + C dissociation.

The remaining part of the exchange nonadditivity consists of the triple-exchange, TE, terms (again with minor contributions from the terms involving multiple exchanges among all three monomers).[35] The TE term is schematically represented by diagram b of Figure 5. It can be obtained by subtracting the SE terms from the overall HL nonadditivity

$$\epsilon_{\mathrm{ex,TE}}^{\mathrm{HL}} \cong \epsilon_{\mathrm{ex}}^{\mathrm{HL}} - \epsilon_{\mathrm{ex,SE}}^{\mathrm{HL}} \quad (9)$$

The full account of higher order corrections that are accessible by means of pseudodimer approach is given after ref 35 in Table 3.

Equations 7 and 8 may be practically applied (in an approximate way) by using standard two-body SAPT codes. The dimer AB is, in this case, described by an SCF wave function (rather than HL one), and the resulting $P_{\mathrm{corr}}$ term also includes the SCF deformation effect. If the latter effect is very small, as, e.g., in rare-gas dimers, one can still obtain reliable estimates of pure exchange contributions. This approach is especially useful if $\epsilon_{\mathrm{corr}}$ is a correction involving an intramonomer correlation effect (such as $\epsilon_{\mathrm{es,r}}^{(12)}$) and the use of the SCF wave function for the AB dimer cannot be avoided.

In Table 4 we list the SE and TE components for several $Ar_2$−molecule systems. One can see that SE and TE are commonly of similar magnitude but differ in sign and thus may largely cancel one another. It is also seen that although $\epsilon_{\mathrm{exch}}^{\mathrm{HL}}$ is the major exchange three-body term, the $\Delta E^{(2)}$ correction, which

**Table 3. Contents of Individual Pseudodimer Contributions in Terms of SAPT Corrections under the Assumption that Induction and Deformation Effects in the Dimeric Subunit Have Been Neglected[a]**

| | |
|---|---|
| $P_{es}^{(10)}$ | |
| $\epsilon_{exch,SE}^{HL}$, all terms | $\Delta E^{HL}$, $\Delta E^{SCF}$ |
| $P_{disp}^{(20)}$ | |
| $\epsilon_{exch-disp,SE}^{(20)}$, selected terms | $\Delta E^{(2)}$ |
| $P_{es,r}^{(12)}$ | |
| $\epsilon_{disp-ind}^{(30)}$ and $\epsilon_{exch-disp-ind,SE}^{(30)}$ (selected terms) | $\Delta E^{(2)}$ |
| $\epsilon_{exch-disp,SE}^{(21)}$ (selected terms) | $\Delta E^{(3)}$ |
| $\epsilon_{exch-coor,SE}^{(12)}$ (selected terms) | $\Delta E^{(2)}$ |
| $P_{disp}^{(12)}$ | |
| $\epsilon_{disp}^{(30)}$ and $\epsilon_{exch-disp,SE}^{(30)}$ (selected terms) | $\Delta E^{(3)}$ |

[a] The supermolecular interaction energies which include individual components are indicated to the right. Note that only selected exchange SE terms are accounted for in the pseudodimer energies, except for the $P_{es}^{(10)}$ case (see the text for details).

in the absence of strong induction is practically determined by the exchange terms (cf. Table 1), is also important.

A pseudodimer approach was also generalized to four-body interactions in the $He_3CO_2$ cluster study.[130]

### 3. Rare-Gas Dimer + Chromophore Clusters

Clusters composed of two rare-gas atoms and a chromophore ($RG_2$−chromophore) represent an excellent paradigm to investigate the complex nature of the three-body interactions. The nonadditive forces may be probed by spectroscopy, and $Ar_2$−HF, $Ar_2$−HCl, and $RG_2$−$CO_2$ have proved to be very useful models. It is also very important that the pair interactions, Ar−Ar, Ar−HF, Ar−HCl, and Ar−$CO_2$, are known with accuracy high enough so that the small three-body interactions could be extracted from spectroscopic measurements. In extending the investigation to more complex systems, $Ar_2$−$H_2O$ comes as a natural next step. The nature of three-body forces in these systems is particularly complex. Therefore, to better appreciate the challenge, we describe below the actual progress in the analytical modeling of the three-body forces in several $RG_2$−chromophore trimers.

### 4. $Ar_2$-HF: Empirical Model vs ab Initio Calculations

When pairwise additivity was assumed, the accurate pair potentials were found to give predicted bending frequencies for the HX (X = F, Cl) hindered-rotation bands of the trimers that were substantially below the measured frequencies.[126,131−134] In addition, the measured red shift for the HF fundamental in the $Ar_2$−HF cluster is 14.827 $cm^{-1}$ (McIlroy et al.[135]), while that calculated for the pairwise-additive potential is 15.355 $cm^{-1}$.[134] The discrepancy of 0.53 $cm^{-1}$ is due mostly to nonadditive forces.

So far, only a family of model three-body potentials of Ernesti and Hutson[132−134] have been constructed and tested against both spectroscopy and ab initio data. These potentials consist of three different terms: dispersion, induction, and short-range component. The most advanced model included the following: (i) A two-site model for the triple dipole *dispersion interaction*; (ii) *induction* dipole moments contributions on the Ar atoms; (iii) the SE term related to the *exchange−quadrupole* of the $Ar_2$ moiety. In addition, Ernesti and Hutson added a dispersion contribution to the $Ar_2$ quadrupole, thus modeling the *induction−dispersion* three-body effect. (iv) The triple exchange (TE) part, dubbed in ref 132 the "exchange overlap" contribution was neglected.

Such model potentials were employed to reproduce the bending levels of $Ar_2$−HX (X = F, Cl) and the red shifts of the HF stretching fundamental. For the bending frequencies of $Ar_2$−HCl, $Ar_2$-DCl, $Ar_2$−HF, and $Ar_2$-DF, Ernesti and Hutson concluded that the most advanced nonadditive model worked reasonably well.[134] The nonadditive contribution to the red shift of the HF stretch in $Ar_2$−HF was only slightly overestimated (15%).[136] For larger clusters, this model potential was similarly successful.[136] However, the recent overtone study by Klemperer's group[137] raised doubts concerning the accuracy of the model potentials in the excited HF stretch ($\nu_{HF} = 3$).

A number of insights into the nature of different three-body contributions in $Ar_2HX$ (X = F,Cl) complexes were provided by a series of ab initio calculations[123,124] (see also refs 34 and 114). The most important finding was that the exchange contribution cannot be faithfully modeled with the exchange-quadrupole term alone. In a very recent study by Kłos et al.,[138] the total ab initio first-order exchange nonadditivity, single and triple exchanges (SE + TE) was calculated on a very large grid of points. In Figure 7, the related surface is compared with the plot of the exchange−quadrupole term. One can see

**Table 4. Comparison of Energy Decomposition (in $\mu E_h$) of Three-Body Terms for the T-Shaped Configurations of the $Ar_2HCCH$, $Ar_2CO_2$, and $Ar_2H_2NCOH$ Clusters and Hydrogen-Bonded Geometries of $Ar_2HX$ Clusters**

| | $Ar_2$−$CO_2$[27] | $Ar_2$−HCCH[128] | $Ar_2$−$H_2NCOH$[129] | $Ar_2$−124HCl[124] | $Ar_2$−HF[124] |
|---|---|---|---|---|---|
| $\Delta E^{SCF}$ | 2.2 | −9.0 | −10.5 | 16.3 | 55.7 |
| $\Delta E^{(2)}$ | 3.1 | 9.2 | 11.2 | 8.3 | −10.0 |
| $\Delta E^{(3)}$ | 22.7 | 24.0 | | 26.3 | 20.2 |
| $\Delta E$(MP3) | 27.9 | 24.2 | | 50.9 | 65.9 |
| $\Delta E^{(4)}$ | | −10.1 | | | |
| $\Delta E$(MP4) | | 14.1 | | | |
| $\Delta E$(CCSD(T)) | | 17.5 | | | |
| $\epsilon_{exch}^{HL}$ | 0.8 | −9.5 | −21.8 | 4.8 | 24.9 |
| SE($Ar_2$−mol) | 9.1 | 1.9 | −14.2 | 27.2 | 43.1 |
| SE | 10.8 | 5.8 | −11.6 | | |
| TE | −8.3 | −15.3 | −10.2 | −23.5 | −20.0 |
| $\Delta E_{def}^{SCF}$ | 1.4 | 0.5 | 11.3 | 11.3 | 30.8 |
| $\epsilon_{disp}^{(30)}$ | 23.3 | 25.8 | 23.0 | 30.6 | 21.5 |

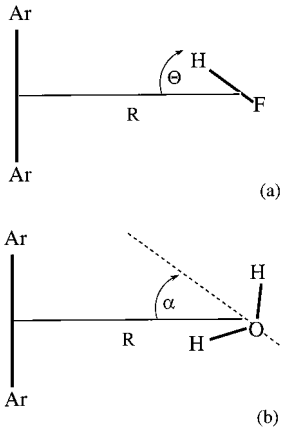


**Figure 6.** Geometries of (a) $Ar_2HF$ and (b) $Ar_2H_2O$.

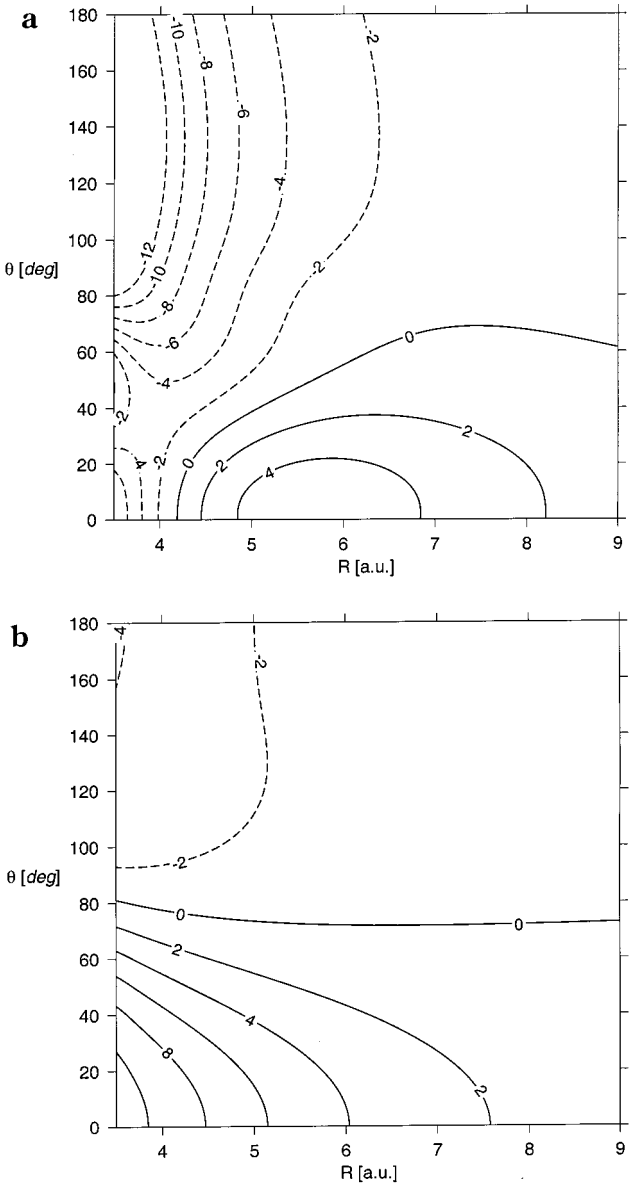


**Figure 7.** Comparison of the $Ar_2HF$ three-body exchange terms from (a) ab initio first-order $\epsilon_{exch}^{HL}$ term[138] and (b) the exchange−quadrupole model of Ernesti and Hutson.[133]

that the total ab initio exchange term is less anisotropic than the exchange−quadrupole effect, especially for small angles Θ. If one replaces, in the Ernesti and Hutson potential, the latter term by the ab initio exchange term (cf. Figure 8), the anisotropy of the total potential for small Θ is significantly mitigated whereas for large Θ the nonadditive potential switches from repulsive to attractive.

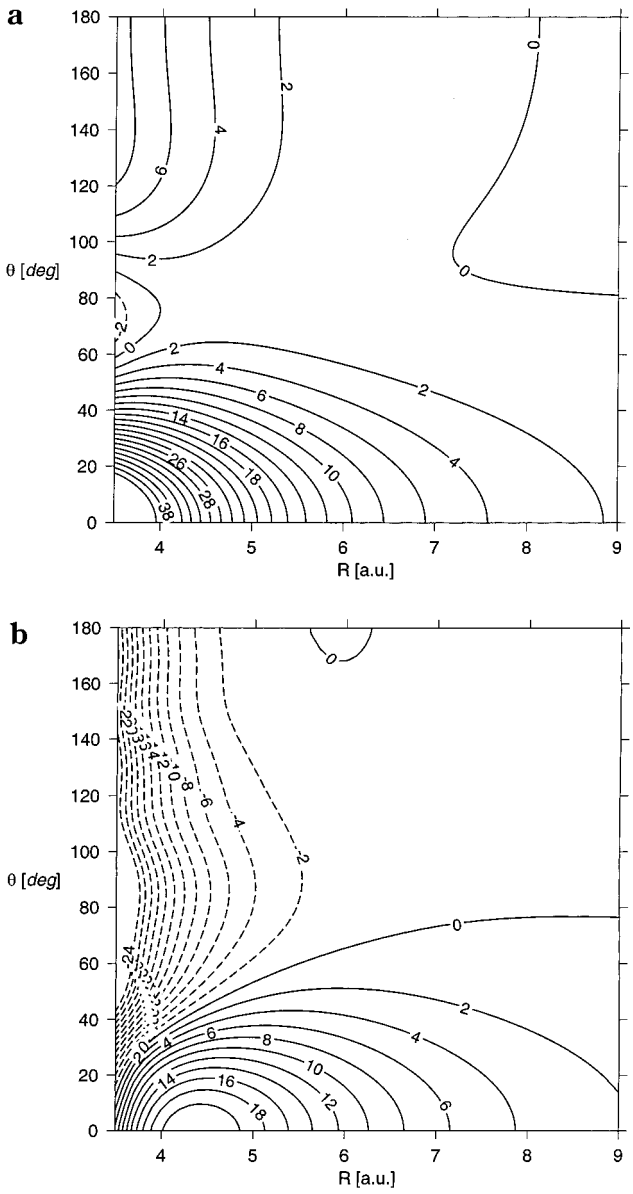


**Figure 8.** Comparison of three-body potentials for $Ar_2$-HF: (a) the original three-body potential of Ernesti and Hutson[134] and (b) the modified Ernesti and Hutson potential with the exchange−quadrupole term replaced by complete first-order $\epsilon_{exch}^{HL}$ term from ab initio calculations.[138]

Several other issues pertaining to ab inito calculations and modeling of the three-body potential in $Ar_2$-HX (X = F,Cl) complexes have been clarified[123,124] and reviewed recently.[21] It was shown that the two dominant exchange contributions, SE and TE, and the major induction component (Ar-induced dipoles interaction) are recovered at the SCF level of theory. At this level the exchange and induction interactions are reproduced with neglect of intramonomer correlation effects. In other words, mutual polarization and electron exchange take place among SCF monomers. The correlation corrections appear first in $\Delta E^{(2)}$ (cf. Table 1).[123,21] These are the exchange−correlation effect and the induction−correlation term along with

its exchange counterpart. The correlation is of the second-order intramonomer type. In addition, $\Delta E^{(2)}$ includes new important nonadditive terms: the exchange−dispersion and induction−dispersion effects. The former proved negligible, but the latter turned out to be very important in the $Ar_2HF$ complex, as shown recently by Lotrich et al.[113,114] Rigorous separation of all these terms is difficult and has not yet been achieved. An explicit expression for exchange−dispersion and induction−dispersion energy was provided in refs 112−114, and the work on the exchange−correlation (intramonomer correlation effect on the exchange repulsion) is in progress.[139,140] Some important insights into the role of exchange−dispersion−induction terms were achieved by means of the pseudodimer approach.[35] On the whole, the $\Delta E^{(2)}$ nonadditivity, although secondary, was found to be important in $Ar_2HX$ (X = F, Cl).[123,21] The next supermolecular three-body correction, $\Delta E^{(3)}$, brings about higher intramonomer correlation corrections and includes a new, dispersion nonadditivity, $\epsilon_{disp}^{(30)}$, related to the well-known Axilrod−Teller−Muto triple-dipole three-body term. $\epsilon_{disp}^{(30)}$ was found to dominate the third-order correlation effect, $\Delta E^{(3)}$, almost completely.

### 5. $Ar_2$–$H_2O$

In extending the investigation to more complex systems, the choice of $Ar_2H_2O$ comes as a natural next step. The interest in $RG_nH_2O$ complexes stems also from the fact that they serve as valuable models for hydrophobic interactions with implications for processes, such as solvation, liquid−liquid interfaces, micelle formation, and biological systems.

Until recently, little was known about small clusters containing Ar/water mixtures other than the single-point calculation of the nonadditive energy contribution for $Ar_2H_2O$.[141] Arunan et al.[142] reported the first observations of rotational spectra of several small clusters: $Ar_2H_2O$, $Ar_3H_2O$, $Ar(H_2O)_2$, and $Ar(H_2O)_3$. In particular, it was concluded that the $Ar_2H_2O$ complex is triangular with the water molecule undergoing virtually free internal rotation. The empirical PES subsequently used[143] for modeling of the $Ar_2H_2O$ spectra indicated a global minimum of $C_{2v}$ symmetry, in contrast to the pairwise additive PES used by Liu et al.,[144] which suggested an asymmetric triangle with the $C_2$ axis of the water molecule roughly perpendicular to the line connecting the center of mass of the water molecule and the center of mass of the argon dimer. This suggested a large role of three-body effects in the structure and dynamics of $RG_nH_2O$ clusters.

Recently, Burcl et al. examined the three-body interactions in the $Ar_2H_2O$ cluster via the calculations carried out through the third order of the MP theory.[145,146] For the sake of presentation, we have selected the coplanar arrangement of the Ar−Ar moiety and the water molecule, with the water monomer undergoing rotation around its center of mass, Figure 6. One can see in Figure 9 that the three-body effects are repulsive for these geometries and show very strong anisotropy. Since these effects are relatively small, amounting to less than 4% of the total interaction energy near the minimum, they should not qualitatively change the behavior of the trimer.

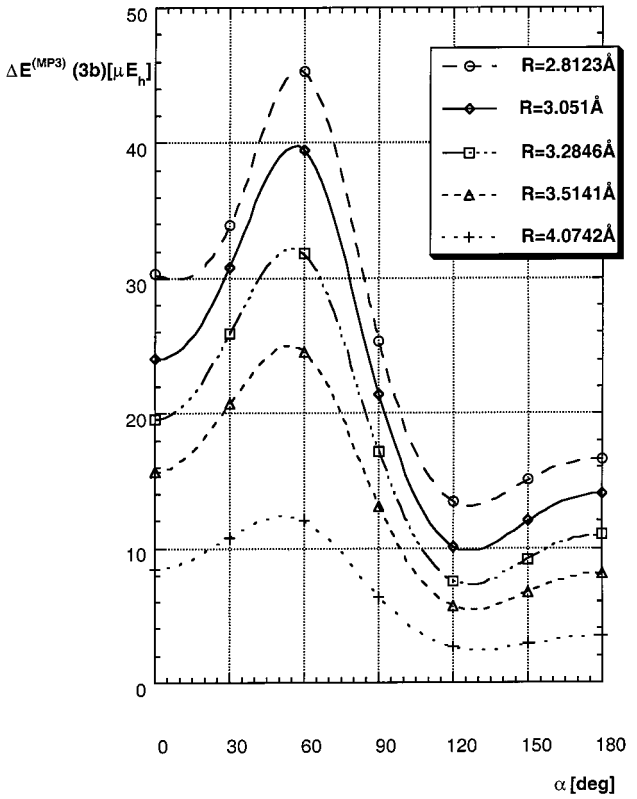


**Figure 9.** Anisotropy of the total MP3 three-body contribution with respect to rotation of water in the $Ar_2H_2O$ cluster (geometry shown in Figure 6b), $R = 2.8123$ Å.[145,146]

The character and decomposition of the three-body term is illustrated in Figures 10 and 11. Similar to the $Ar_2HX$ complexes, there is no dominant term and the overall magnitude and anisotropy of the three-body effect results from a fine balance of various terms.

The terms contributing to the SCF nonadditivity are shown in Figure 10. The $\epsilon_{exch}^{HL}$ term is decomposed into the single exchanges (SE) term (which is dominated by the electrostatic $Ar_2$ exchange−quadrupole interaction with the water molecule) and the triple exchanges (TE) term. SE is the most anisotropic, but TE largely cancels this anisotropy in the 0°−90° region, and enhances it in the 90°−180° region. The third SCF component, the induction nonadditivity, as represented by $\Delta E_{def}^{SCF}$, is generally smaller than the exchange contribution but quite anisotropic and certainly nonnegligible in the context of the total effect.

The $\Delta E^{(2)}$ three-body term is large (often larger than $\Delta E_{def}^{SCF}$) but not very anisotropic (cf. Figure 11). It includes the exchange−dispersion and exchange−correlation components. This term also includes the induction−correlation and induction−dispersion terms, both strongly affected by exchange effects (cf. Table 1). Some of these terms are reproduced by the pseudodimer calculations. $P_{disp}^{(20)}$ includes SE−exchange−dispersion. $P_{es,r}^{(20)}$ includes induction−dispersion along with its SE−exchange counterpart, correlated SE−exchange−dispersion and SE−ex-

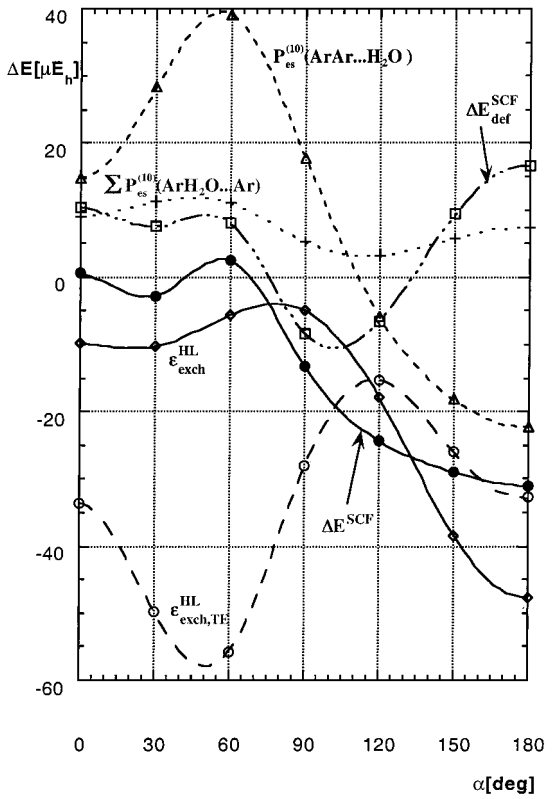


**Figure 10.** Anisotropy of terms contributing to the SCF nonadditivity with respect to the rotation of water in the $Ar_2H_2O$ cluster (geometry shown in Figure 6b), $R = 2.8123$ Å.[145,146]

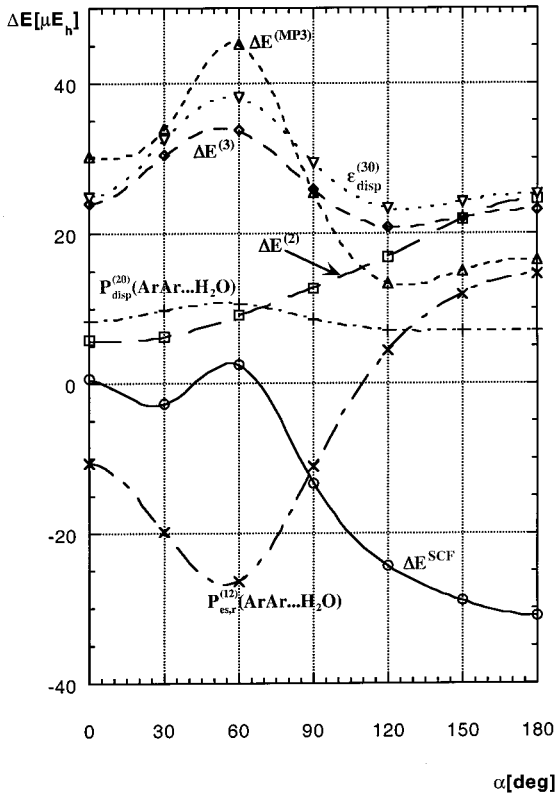


**Figure 11.** Anisotropy of the post-SCF nonadditive terms with respect to the rotation of water in the $Ar_2H_2O$ cluster (geometry shown in Figure 6b), $R = 2.8123$ Å.[145,146]

change−correlation. Still, the anisotropy of $\Delta E^{(2)}$ is not fully recovered. It is clear, however, that in order to approximate the overall nonadditivity in the $Ar_2H_2O$ cluster, the $\Delta E^{(2)}$ contribution is indispensable.

The $\Delta E^{(3)}$ nonadditivity mostly follows the $\epsilon_{disp}^{(30)}$ term, suggesting that higher order induction, exchange, and mixed terms are either mutually canceled or secondary in importance (cf. Figure 11). Since there is a great deal of cancellation between the SCF and $\Delta E^{(2)}$, the three-body dispersion term, $\epsilon_{disp}^{(30)}$, appears to be largely responsible for the dependence of the overall three-body effect on the shape of the Ar−Ar−water triangle.

### 6. $Ar_2CO_2$: Nonadditivity of the Red Shift

In $Ar_2CO_2$, Nesbitt's group observed the nonadditivity of the red shifts associated with the asymmetric $CO_2$ stretch.[147] In this cluster, both pair Ar−$CO_2$ interactions are completely equivalent; therefore, any departures from the additivity of shifts due to Ar−$CO_2$ interactions are essentially attributable to the three-body effects. The observed nonadditivity of this shift was a minute 0.042 $cm^{-1}$.[147] Rak et al.[27] calculated the three major components of the nonadditive interaction as functions of the $CO_2$ asymmetric stretch and evaluated the shift using a one-dimensional vibrational model. Their predictions came within a remarkable 10% of the observed shift. It was found that the induction nonadditivity made the largest positive contribution to the shift's nonadditivity, which was caused by the appearance of the dipole moment (and higher, odd-rank multipoles) in the deformed $CO_2$ molecule. This effect was counterbalanced by negative contributions from the exchange and dispersion interactions. The model properly representing the coordinate-dependence of the three-body potential was the three-body analogue of the simple SCF + dispersion approach. Interestingly, the simplicity of this model may be contrasted with the fact, also shown in this paper, that one needs CCSD(T) in describing the analogous dependence of the two-body potential[27] (see above section III.A.1).

### 7. $Ar_2Cl^-$

$Ar_2Cl^-$ serves as an important model in the study of ion solvation. The study of $Ar_2Cl^-$ was one of the earliest to examine nonadditive interactions by means of the ab initio supermolecular MP3 and intermolecular perturbation approaches.[148] When the pair separations are close to or larger than the equilibrium distances, the three-body effect is well approximated by the induction component, related to the interaction of charge-induced dipoles at the Ar atoms. At closer approach, the HL term begins to dominate and both the $\Delta E^{(2)}$ and dispersion nonadditivities become substantial. Both single exchanges (SE) and triple exchanges (TE) terms are large, and the former was well approximated by an electrostatic interaction between a charge and the exchange−quadrupole on $Ar_2$. The dispersion term is reasonably well approximated by the dipole−dipole−dipole and dipole−dipole−quadrupole components.

An elaborate empirical model, in the same spirit as discussed for $Ar_2HX$[133] and $Ar_2Cl^-$,[148] was recently proposed for $Ar_2Br^-$ and $Ar_2I^-$ by Yourshaw et al.[149]

The nonadditive terms proved crucial to obtain electron affinities consistent with the experimental observations. The major contribution originated from the induction forces, but the exchange and dispersion terms considerably improved the agreement.

## C. Open-Shell Clusters

### *1. Nature of Interaction in Open-Shell Clusters*

One of the ongoing challenges in the study of intermolecular forces is to gain insights into the nature of open-shell van der Waals complexes (see refs 150 for recent reviews). There is a growing interest in these complexes for two reasons: (i) their interactions are viewed as intermediate between the nonbonding van der Waals interactions and the chemical bonding[8] and (ii) many of them are prereactive complexes formed in the entrance valleys of reactive potential-energy surfaces. There is increasing evidence that these complexes can profoundly affect the outcome of reactive events.

The remote regions of the reactive potential surfaces are governed by the long-range forces. These forces have a capacity for orienting the reactants favorably or unfavorably as they approach one another or may trap them in potential wells before they have a chance to engage in reactive encounters. Dubernet and Hutson[151] postulated that such long-range potential wells, which can support bound or quasibound van der Waals states, can exist for any reaction unless the process occurs without a potential barrier. The dramatic effects of the entrance−channel complexes on the reaction outcome were demonstrated recently by Skouteris et al.,[9] who found that weak interactions which lead to the formation of Cl−HD open-shell van der Waals complex in the reactant channel of the Cl + HD($v = 0$) reaction cause a strong preference for the production of DCl over HCl. They state unequivocally "The study of chemical reaction dynamics has now advanced to the stage where even comparatively weak van der Waals interactions can no longer be neglected in calculations of potential energy surfaces of chemical reactions".[9] The studies of the entrance−channel complexes carry another promise: The information about their bound states can be used to gain control over the reaction. One way to induce the reaction within the prereactive complex would be to selectively excite the vibrational states of monomers.[152,153] The other, as postulated by Anderson et al.,[154] would be to excite the intermolecular vibrational modes so that the complex could sample the configurations which are close to the transition-state structure for the reaction.

The interactions involving an open-shell moiety are, in principle, more anisotropic than closed-shell interactions. The presence of unpaired electrons induces a new type of electronic anisotropy which leads to the description of intermolecular forces in terms of manifolds of potential-energy surfaces.[155] The electronic anisotropy is further complicated by several sources of the angular momentum in these systems. These include angular momenta due to the spin and orbital motion of unpaired electrons, monomer rotations, and the rotations of the complex as a whole. The spin−orbit coupling leads to an additional splitting into an even larger manifold of surfaces. Open-shell reactants also open up reactive channels on the PESs which further affect their shapes and their mutual interactions.

Ab initio modeling of these multisurface interactions is a difficult task because the standard methods designed to treat closed-shell complexes, such as size-consistent single-reference methods based on Møller−Plesset or CC theories, may not be applicable. The consensus today is that these calculations should involve highly correlated multireference approaches employing very large orbital basis sets.[100] However, attempts to apply the multireference methods, such as generalized valence bond (GVB), complete active space self-consistent field (CASSCF), and complete active space perturbation theory (CASPT2/3), multireference configuration interaction (MRCI), to the open-shell van der Waals interactions are also plagued with problems. The CASSCF and MRCI are not size-extensive and require size-consistency corrections which are always approximate. In addition, size-inconsistency prevents one from using the straightforward CP corrections for BSSE. Even if size-consistent methods are used, the removal of BSSE is difficult because in the multisurface case there are many different counterpoise monomer states (see section III.C.3).

In some instances the adiabatic PESs may interact with one another giving rise to nonadiabatic coupling effects.[156] In such circumstances the transformation of the adiabatic solutions to an approximate diabatic basis is necessary (see section III.C.2).

One of the most accurate single-reference approaches is an open-shell coupled-cluster treatment with single, double, and noniterative triple excitations. This approach can be applied in the spin-unrestricted (UCCSD(T)) or partially spin-restricted (RCCSD(T)) variants. It is size-extensive and due to the inclusion of triple excitations, highly suitable to treat the dispersion-bound complexes. Its applicability is, however, limited to open-shell complexes when the monomers can be identified and well separated. This approach was applied successfully in the studies of a number of van der Waals complexes of the RG-open-shell atom and RG-open-shell molecule type.[11,22,96,157−162] Both RCCSD(T) and MRCI were used for the prereactive complexes, $B-H_2$[163] and $O-H_2$.[10]

The interpretation of the supermolecular UCCSD(T) results was greatly enhanced by the recently proposed and implemented generalization of the symmetry-adapted perturbation theory to open electron shells by Cybulski et al.[164] Within the framework of the Møller−Plesset partitioning of the Hamiltonian, two perturbations were defined: the interaction operator and intramonomer correlation operator. The unperturbed wave function $\Psi_o$ was represented as a product of the UHF monomer wave functions, and the energy terms were evaluated for all possible spin combinations (see ref 164 for details). The electrostatic ($\epsilon_{es}^{(10)}$), HL-exchange ($\epsilon_{exch}^{HL}$), induction ($\epsilon_{ind,r}^{(20)}$), dispersion ($\epsilon_{disp}^{(20)}$), and electrostatic-correlation ($\epsilon_{es,r}^{(12)}$) terms were implemented.

The insights gained from these calculations will be discussed below in Section D for a few typical van der Waals complexes between rare gases and open-shell atoms/molecules, as well as a prereactive complex of a $^2$P state atom with a molecule, Cl + HCl.

### 2. Adiabatic vs Diabatic Solutions

Ab initio calculations of open-shell complexes usually lead to a manifold of adiabatic states, $\{\Psi_i^a\}$. The adiabatic representation, due to noncrossing rule, often results in significant couplings between the nuclear and electronic motions, especially around avoided crossings. Such states are a poor choice for nuclear dynamics calculations. It is thus necessary to transform them into a diabatic basis, $\{\Psi_i^d\}$ in which the states are allowed to cross and these couplings vanish. Diabatic states can be related to the adiabatic states by a unitary transformation

$$\Psi_i^d = \sum_j \Psi_j^d U_{ji} \tag{10}$$

where $U$ is chosen from the criterion

$$\langle \Psi_j^d | \partial/\partial q | \Psi_i^d \rangle = 0 \tag{11}$$

for all the coordinates $q$. Unfortunately, in the multidimensional case this problem cannot be solved uniquely.[156,165] This necessitates the use of *approximate*, i.e., quasi-diabatic states. A variety of such approaches has been proposed in the literature. In the case of two interacting states of the same symmetry, the transformation $U$ is represented by a $2 \times 2$ rotation around a single "nonadiabatic mixing angle" $\gamma$. As shown by Rebentrost and Lester,[166] the $\gamma$ angle can be obtained from matrix elements of the electronic angular momentum. Alexander[10,163] evaluated these matrix elements for the MRCI wave function. An alternative "direct" diabatization based on the analysis of the CI wave function was proposed by Werner et al.[167] It is worth noting that the resulting diabatic states are no longer eigenvectors of the electronic Hamiltonian which gives rise to an extra coupling term. Thus, in a two-state case, transformation to a diabatic representation leads to three diabatic states. This third "state" must be included in bound-states calculations of open-shell clusters.[151]

### 3. Treatment of BSSE in Open-Shell Clusters

The calculations of interaction energies in open-shell clusters can be accomplished via the CP procedure, which is in many respects similar to the closed-shell case provided size-extensive methods are used. An application of this procedure, however, is more involved because these interactions are represented by more than one PES. Simultaneously, the monomer state may split, as symmetry is usually lowered in the dimer basis set by the presence of ghost orbitals, into what one may call the *monomer counterpoise states*. If there is only one state of a given symmetry, the monomer CP states can be easily correlated with the appropriate dimer states. For example, the two monomer counterpoise states of a $^2$P atom approaching a linear molecule along its $C_\infty$ axis are $\Sigma$ and $\Pi$. These monomer states can be correlated with the $\Sigma$ and $\Pi$ states of the dimer.

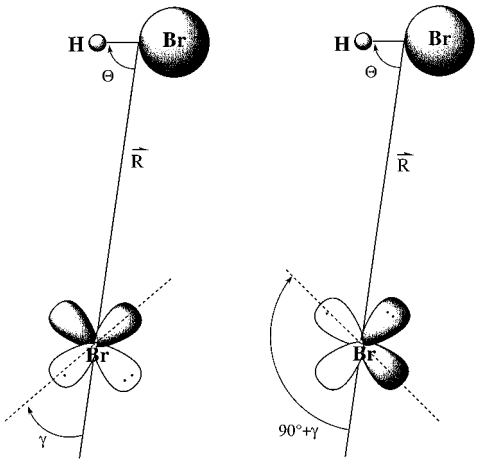


**Figure 12.** Schematic representation of two different states of the A′ symmetry in $^2$P atom + linear molecule interaction. The two states can be (approximately) distinguished by two orthogonal orientiations of the singly occupied p orbital of an atom.

If there are two states of the same symmetry, a task correlating the dimer states with the appropriate monomer states, although less routine, is still possible. Let us consider a following example involving a $^2$P atom and a linear molecule, HBr + Br($^2$P), in a nonlinear $C_s$ configuration. The HBr + Br($^2$P) interaction in such an arrangement gives rise to two A′ states. These states can be schematically depicted (see Figure 12) as two orthogonal orientations of the singly occupied 4p orbital of Br with respect to HBr. A similar analysis of the monomer states allows us in many instances to match the dimer states with the appropriate monomer states. If there is some ambiguity in such an assignment, it can be removed upon transformation to an approximate diabatic representation. Alexander details such a CP procedure for approximate diabatic solutions for the $H_2$ + B($^2$P) complex.[163] Thus, the CP correction can be performed either before[168] or after diabatic transformation.[163]

How important is correcting for BSSE in a multisurface case? In the discussed example of HBr + Br($^2$P), there are three PESs, 1A′, 2A′, and 1A″. In Figure 13a the angular cuts through the adiabatic total dimer PESs and the analogous cuts through the CP-corrected interaction energy surfaces (Figure 13b) are displayed.[169] One can see that the dimer curves which are contaminated by BSSE have different shapes than the BSSE-free interaction energy curves. In particular, the 2A′ dimer curve reveals a peculiar negative second derivative at $\Theta = 0°$. Moreover, the 2A′−1A′ splitting is incorrectly represented by the dimer curves.

The use of non-size-extensive approaches, such as multireference CI, in the treatment of open-shell clusters brings about another difficulty. In this case the straight application of Boys and Bernardi CP recipe leads to meaningless results,[170] even if standard size-consistency corrections such as Davidson's or Pople's are included. This is because the monomer

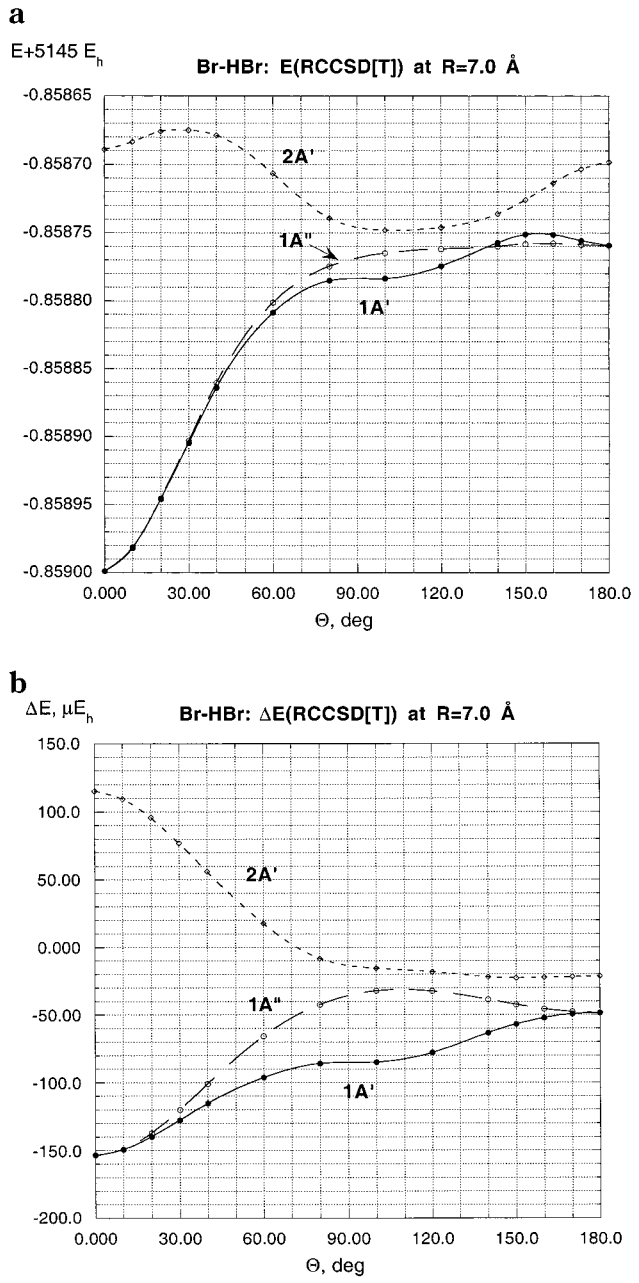


**Figure 13.** Adiabatic 1A′, 2A′, and 1A″ states of the HBr + Br($^2$P) complex at $R$ = 7.0 Å plotted as a function of Jacobi angle Θ: (a) total CP-uncorrected states; (b) CP-corrected interaction energies. To facilitate the comparison, the scale of the graphs in a and b is the same. The calculations were carried out at the RCCSD[T]/aug-cc-pVTZ+bf(332) level of theory.[169]

is described by a poorer *many-electron basis set* (poorer set of configuration states) than the dimer, even if a full dimer *one-electron basis set* is used to build configurations. This gives rise to an additional basis-set superposition error related to the inconsistency in the many-electron basis set for the monomers and the complex.[171] This error was dubbed the "configuration state superposition error" by van Duijneveldt et al.[4] Removing such an inconsistency is anything but trivial (cf. refs 4 and 172). Faced with this difficulty, a common practice is to neglect the BSSE correction altogether, counting that this error is small, and correcting only for size-extensivity effects.[10,100,173,174] However, such a tactic may preclude the usage of basis sets that are very efficient in interaction calculations but produce large BSSE, such as basis sets with bond functions.

## D. Model Calculations

### 1. Ar–OH($X^2\Pi$): A Paradigm

The importance of a hydroxyl radical stems from its ubiquity in atmospheric chemistry[175] and combustion processes. It is involved in many hydrogen abstraction reactions which include oxidation of $H_2$, $CH_4$, and a variety of hydrocarbons. The $H_2 + OH \rightarrow H_2O + H$ reaction is one of several possible models for such reactions. A useful probe of the entrance channel of this process is provided by the interaction of OH and a rare-gas atom. The advantage of the latter is that it can be characterized at a high level of accuracy.

Over the past decade there has been a great deal of experimental and theoretical interest in the open-shell system Ar−OH.[176−184] Its ground state, Ar−OH($X^2\Pi$), has been thoroughly characterized by the stimulated emission pumping (SEP) technique.[176−178] Using SEP, Lester and co-workers identified virtually all of the bound vibrational levels of Ar−OH($X^2\Pi$), from the zero-point level to the dissociation limit. In addition, many metastable levels have been detected as much as 200 cm$^{-1}$ above the OH ($X^2\Pi$) + Ar dissociation limit. These data sampled a considerable portion of the intermolecular PES.[178,179] The inversion of these data have led Dubernet and Hutson[179] to the first reliable semiempirical potential of Ar−OH($^2\Pi$).

The first ab initio PES for Ar−OH($^2\Pi$) was assembled by Degli Esposti and Werner on the basis of the coupled electron pair approximation (CEPA) calculations.[180] This PES, which in the early 1990s represented the state of the art, was subsequently used to simulate the electronic and rovibrational spectra.[185−187]

Recently, Kłos et al.[22] calculated the adiabatic PESs for the $^2$A′ and $^2$A″ states of the Ar−OH(X $^2\Pi$) complex, by means of the supermolecular UMP4 method using a large correlation-consistent basis set supplemented with bond functions (aug-cc-pVTZ + bf(332)). The PES of the A′ state has two minima. The global minimum at the UMP4 level of theory occurs for the collinear geometry Ar−H−O at $R$ = 7.08 $a_0$ with a well depth of $D_e$ = 141.2 cm$^{-1}$. There is also a local minimum for the skewed T-shaped form, whereas the Ar−O−H arrangement corresponds to a saddle point. The PES of the A″ state also has two minima, which occur for the two collinear isomers.

The UMP4 potential reproduced the experimental energy levels from SEP[176,177] and IR[188] measurements to within the experimental accuracy in most cases, cf. Figure 14. The van der Waals stretching energies, which were underestimated by the CEPA potential, have been correctly (to within 3% of the experimental values) predicted by the UMP4 potential. The most notable difference between experimental and calculated energies occurred at the first excited bend which was experimentally predicted at 9.2 cm$^{-1}$ vs the ab initio value of 10.8 cm$^{-1}$. This discrepancy

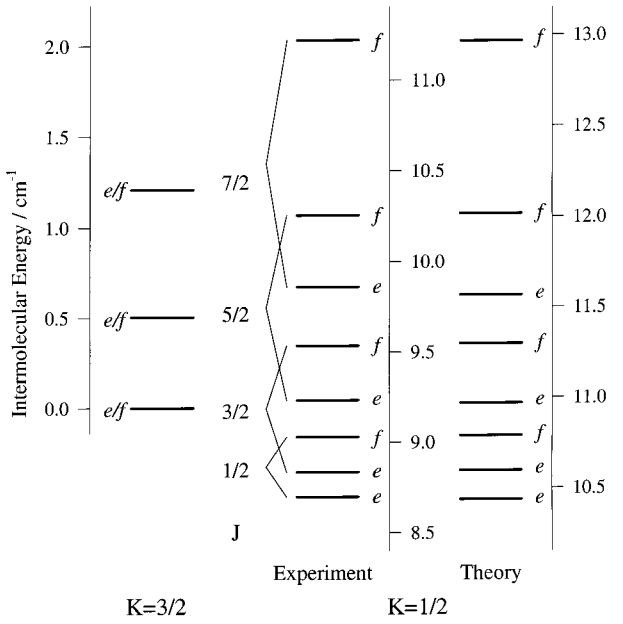


**Figure 14.** Rotational energy level diagram for ArOH ($\nu_{OH} = 1$) in the lowest intermolecular state ($P = {}^3/_2$) and excited intermolecular bending state ($P = {}^1/_2$) that have been accessed experimentally.[188] Also shown for comparison are the rotor levels computed for the $P = {}^1/_2$ bending state of ArOH ($\nu_{OH} = 0$) using the UMP4 potential.[22] Only the intermolecular energy is plotted, with the zero of energy defined at the $J = {}^3/_2$, $P = {}^3/_2$ state (parity averaged). Both experiment and theory show large splitting between e/f parity components of a given rotor level in the $P = {}^1/_2$ state, while no parity splitting is observed for the $P = {}^3/_2$.

suggested that the UMP4 potential was slightly too anisotropic between 0° and 90° in the range of $R$ sampled by $|\nu_s = 0\rangle$. Interestingly, the CEPA potential performed better for this bend providing 9.2 cm$^{-1}$.

The parity splitting (of the $J = {}^3/_2$ level of the $|\nu_s = 0\rangle|\nu_b = 1\rangle$ state) predicted by the UMP4 potential was 0.67 cm$^{-1}$. The CEPA potential predicted a splitting of 0.58 cm$^{-1}$.[179] The semiemperical potential of Dubernet and Hutson[179] reproduced the previously reported experimental value of 0.23 cm$^{-1}$ to which it was fit. However, Dubernet and Hutson found it difficult to reconcile this small splitting with the reported magnitude of the parity splitting in the ground vibrational state.[179] Recent experiments by Bonn et al.[188] showed that the earlier experimental value was in error and that the correct splitting for this level is 0.69 cm$^{-1}$, in good agreement with the UMP4 value.

The UMP4 potential has also been used recently in quantum scattering calculations by van Beek et al.[189] to interpret their recent experiments on rotationally inelastic collisions of OH($X^2\Pi$) + Ar. For the state-to-state cross sections, the overall agreement between experiment and theory was very good to excellent, particularly for spin−orbit conserving transitions.[189a] For the effects of molecular orientation the UMP4 potential yielded excellent predictions for transitions to states of A″ symmetry and good for transitions to states of A′ symmetry.[189b]

The very good agreement between theory and experiment achieved for OH($X^2\Pi$) + Ar represents an example of what may be expected from ab initio methods for other open-shell complexes of a comparable size and a similar nature.

### 2. He–CH($X\ ^2\Pi$): Incipient $\pi$ Bond

van der Waals interactions of the CH radical in its ground $X\ ^2\Pi$ electronic state have attracted a lot of interest.[159,190−193] The study of the reaction of CH and $H_2$ is of special importance because it is the simplest reaction in carbyne−alkane chemistry. The CH + He interaction may be viewed as a nonreactive analogue of CH + $H_2$.

The $X\ ^2\Pi$ state of CH is of great theoretical interest, since the two states arising from the interaction of the singly occupied $\pi$ orbital with a RG atom differ dramatically from each other. The $X\ ^2\Pi$ state of CH corresponds to the $1\sigma^2 2\sigma^2 3\sigma^2 1\pi^1$ configuration and gives rise to two electronic states of the CH−He complex, $^2$A′ and $^2$A″,[191] related to two different orientations of He with respect to the singly occupied $1\pi$ orbital of CH.

The detailed ab initio description of the PESs of He−CH($^2\Pi$) was given in ref 159. The A′ PES represents a typical van der Waals interaction which is characterized by two similarly deep minima. The first minimum occurs for the collinear He−C−H arrangement, at $R \approx 7.5\ a_0$ and $\Theta = 0°$ and is 55 $\mu E_h$ deep. The second minimum has a trough-like form joining the region between $R = 7.5\ a_0$, $\Theta = 140°$ and $R = 8.0\ a_0$, $\Theta = 180°$. The lowest point is approximately 54 $\mu E_h$ deep and occurs at $R = 7.5\ a_0$ and $\Theta = 140°$. The shape and location of these minima are determined primarily by the anisotropy of the dispersion component.

In contrast, the A″ state PES has only a single and relatively deep minimum of $D_e \approx 335\ \mu E_h$ for the T-shaped geometry, at $R = 5.0\ a_0$ and $\Theta = 100°$. The minimum is unusually deep for a complex involving He.

Why is state A″ so different from A′? In the A′ state, the singly filled CH $\pi$-orbital lies on the molecular plane facing the He atom. This arrangement results in a considerable exchange repulsion. In the A″ state, this repulsion is drastically reduced because He faces a nodal plane of this $\pi$-orbital which in this state is perpendicular to the molecular plane. Due to the weak repulsion, He could approach more closely and experience stronger binding. Reduced repulsion also directs He toward a T-shaped structure rather than to a H-bonded one. This unusually deep minimum with $D_e = 335\ \mu E_h$ may be compared with that for a relatively strong complex He−HF with $D_e = 179\ \mu E_h$.[84] The reduction of repulsion for the T-shaped configuration has been observed for several other RG−diatom complexes (RG−CO,[194] RG−$Cl_2$,[195] RG−$O_2$,[196] etc.), yet in this particular case it is untypically large. It is best demonstrated in Figure 15 by plotting the ratio of $\epsilon_{disp}^{(20)}/\epsilon_{exch}^{HL}$ and $\Delta E_{def}^{UHF}/\epsilon_{exch}^{HL}$. The first of these ratios reveals an unexpected dip around 100°. It is clear that something happens there which has to do with the sudden drop in the HL-exchange repulsion. One may view this effect as the incipient chemical bond formation. Since it conserves the $\pi$ nodal plane, it may be dubbed an "incipient $\pi$ bond".

Another example of such an incipient $\pi$ bond was reported for the He($^1$S)−Li($^2$P) complex by Bililign et

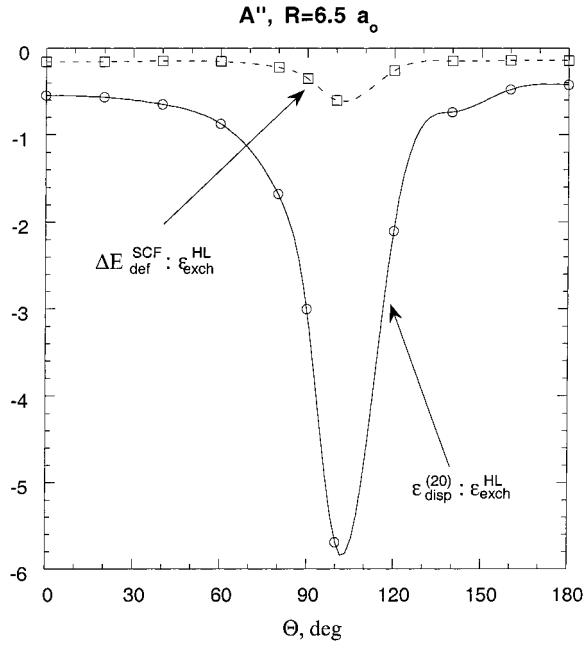


**Figure 15.** Angular dependence of the ratios: UHF deformation against HL exchange and dispersion against HL-exchange energies for the $^2A''$ state of the He−CH($X^2\Pi$) complex:[159] (---) $\Delta E_{def}{}^{UHF}/\epsilon_{exch}{}^{HL}$, (—) $\epsilon_{disp}{}^{(20)}/\epsilon_{exch}{}^{HL}$.

al.[197] This complex displays an anomalously reduced repulsion compared to Ne($^1$S)−Li($^2$P). The authors argued that when the 1s orbital of He approaches the nodal plane of a perpendicular 2p orbital of Li, the exchange repulsion is reduced due to the vanishing intermonomer overlap integral. At the same time, the overlap argument does not apply to the dispersion interaction (which is represented by simple two-electron integrals) and the dispersion interaction between these orbitals is not affected.

### *3. ArO−: Electron Photodetachement Spectrum*

A study of open-shell complexes is not complete unless the spin−orbit coupling is taken into account. However, a relativistic treatment is highly nontrivial, and there are very few studies which meet the challenge of even approximately including these effects. The study of ArO and its anion provides an example of how accurate ab initio nonrelativistic adiabatic potentials can be combined with a relativistic model of atoms-in-molecules (AIM) to provide reliable simulations of the photoelectron spectra. Such spectra were recorded by Bowen et al.[198,199] and reproduced from ab initio calculations by Buchachenko et al.[11]

As far as the adiabatic potentials are concerned, ab initio results reveal that the complex of Ar with atomic oxygen is only weakly bound, primarily by dispersion interaction. The Π state possesses a deeper minimum ($R_e$ = 3.4 Å, $D_e$ = 380 $\mu E_h$) than the corresponding Σ state ($R_e$ = 3.8 Å, $D_e$ = 220 $\mu E_h$). The Σ−Π splitting is mainly due to differences in the exchange repulsion terms. The Π state is related to the single electron contact and thus may be viewed as an incipient chemical bond. The Σ state reveals a van der Waals binding.

In contrast, the complex of Ar with the oxygen anion is fairly strongly bound, primarily by ion-

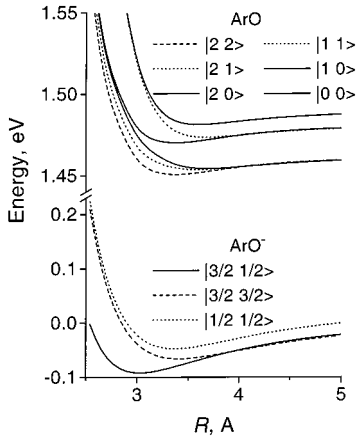


**Figure 16.** Relativistic potentials of $ArO^-$ and ArO from the relativistic "atoms-in-molecule" approach and from UMP4 calculations.[11] Atomic limits are, in ascending order, $j^- = {}^3/_2$, ${}^1/_2$ and $j$ = 2, 1, 0.

induced dipole induction forces, and the Σ state possesses a deeper minimum at shorter interatomic distances ($R_e$ = 3.02 Å, $D_e$ = 3600 $\mu E_h$) than the corresponding Π state ($R_e$ = 3.35 Å, $D_e$ = 2400 $\mu E_h$). The Σ−Π splitting is again due to differences in the exchange repulsion terms. Here, the Σ state is related to the single electron contact and thus may be viewed as an incipient chemical bond. The Π state reveals a van der Waals character. By combining the adiabatic curves with the AIM approach, a larger manifold of six ionic/neutral states is obtained, cf. Figure 16.

For the quantitative spectrum simulations, a refined vibronic model was used in which the transition energy was given as the difference of the accurate vibrational term values for particular anion and neutral states. The transition intensities were obtained by a sum of vibronic factors (cf. ref 11 for details).

The deep potential wells of anion states support many vibrational levels, among which up to 10 were retained for spectrum simulations. The shallower neutral curves support only four or five levels. Transitions to all of them were considered. The simulated spectra from ref 11 are compared with measured ones[199] in Figure 17. The experimental spectra exhibit poor structure with only two closely spaced peaks, designated as "X" and "A", being resolved (the left and right peaks in Figure 17, respectively). The theoretical model reproduces very well the spectral shapes at quite realistic temperatures 75−100 K. At low temperature, the peak X, composed of the transitions from the ground $X_{1/2}$ state of anion, dominates. The transitions from the second anion state $I_{3/2}$, which form peak A, are more intense, but manifest themselves only as a shoulder (due to weak population). At a high temperature, the population of the $I_{3/2}$ state becomes large enough to make the A peak dominate and absorb the X peak. At an intermediate temperature, both peaks are of the same height and the intensity distribution becomes bimodal. To summarize, the most important result of this simulation is the prediction of strong selectivity of spin−orbit transitions.

It should be emphasized that these features of the photoelectron spectrum are completely determined

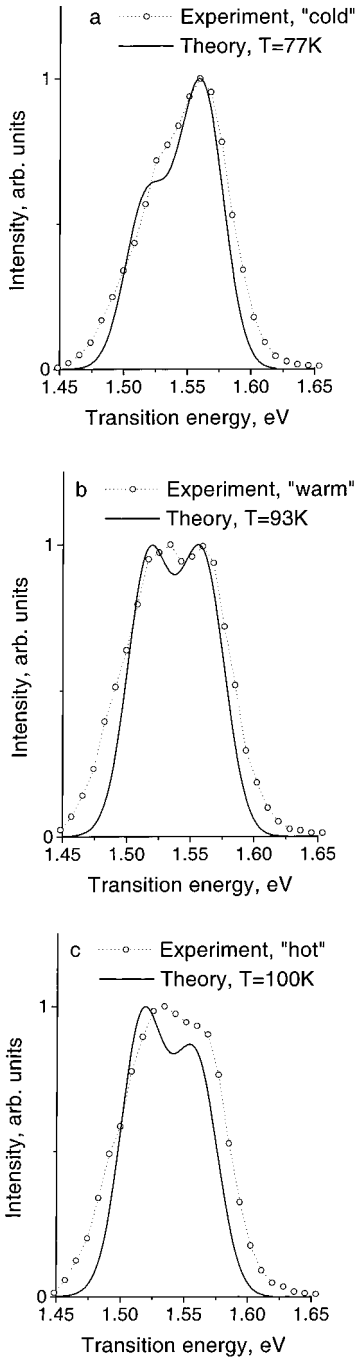


**Figure 17.** Photoelectron spectra of $ArO^-$ at (a) "cold", (b) "warm", and (c) "hot" conditions. Experimental data are taken from ref 199. Simulations were performed using the vibronic model of ref 11. Left and right peaks are referred to in the text as the "X" and "A" peaks, respectively.

by the electronic intensity factor. The simulations which neglect the electronic contribution and estimate the transition intensity through the simple vibrational Franck−Condon factor predict structureless single-peak intensity distribution over the wide range of vibronic temperatures.

### *4. Prereactive Complex: Cl($^2$P) + HCl*

The Cl + HCl → ClH + Cl reaction is an important prototype of a heavy−light−heavy atom-exchange process. It is also a typical reaction which takes place on multiple, coupled potential surfaces. The ab initio modeling of the potential surfaces has concentrated primarily upon the transition-state region, with much less attention devoted to the van der Waals region. Recently, Dobbyn et al. carried out high-quality calculations combining RCCSD(T) and MRCI for the reactive region of the PES.[200] In the reactant valley, there exists a reasonably deep well which can trap the Cl($^2$P) and HCl reactants. Wittig's group recently generated the Cl−HCl entrance−channel complex by photodissociation of $(HCl)_2$ and expressed the hope of soon achieving sufficient resolution to measure its spectrum.[201] Prior to our very recent work,[168] the only information on this van der Waals well came from Dubernet and Hutson, who combined the multipole-expanded electrostatics with the semiempirical Ar−Cl($^2$P) and Ar−HCl potentials, from which they extracted only the appropriate parameters.[202] This approach provided the three empirical adiabatic states which were used to predict the spectral range where the stretching and bending frequencies should occur.[202]

From the ab initio standpoint, the Cl($^2$P) + HCl interaction represents a serious challenge. The electron configuration of Cl gives rise to two states of $^2$A′ symmetry and one of $^2$A″ symmetry for the bent geometries and to $^2\Sigma$ and $^2\Pi$ states in the collinear arrangement. Kłos et al. calculated the three adiabatic, $1^2$A′, $2^2$A′, and $1^2$A″ PESs (see Figure 18a−c), employing the RCCSD(T)/aug-cc-pvtz + bf(332) level of theory.[168] The reference function was obtained from the spin-restricted RHF calculations. The reference for the $2^2$A′ state was obtained by 90° rotation of the singly occupied orbital.

It is interesting to compare the features of the adiabatic ab initio PESs with those of the empirical surfaces of Dubernet and Hutson (see Table 5). The $1^2$A′ surface displays a global minimum with $D_e$ = 625 cm$^{-1}$ for a T-shaped structure and a secondary one with $D_e$ = 442 cm$^{-1}$ for a collinear Cl−HCl orientation. The empirical surface also has the T-shaped and linear minima, but their well depths are very close (347 vs 383 cm$^{-1}$, respectively). The $1^2$A″ surfaces from both approaches are very similar. Namely, the ab initio surface contains the global collinear Cl−HCl minimum ($D_e$ = 442 cm$^{-1}$) and a secondary collinear Cl−Cl−H minimum ($D_e$ = 174 cm$^{-1}$). The empirical surface features the same minima with $D_e$ = 383 and 200 cm$^{-1}$, respectively. In contrast, the $2^2$A′ surface differs somewhat in both approaches. While the ab initio calculations provide the minimum for a linear Cl−Cl−H structure ($D_e$ = 128 cm$^{-1}$), the empirical surface provides a shallow ($D_e$ = 50 cm$^{-1}$) quasi-linear Cl−Cl−H minimum.

The Cl atom in the $^2$P state possesses an appreciable quadrupole moment. Thus, the electrostatic energy of the Cl−HCl complex displays a long-range, quadrupole−dipole asymptotic behavior. The ab initio electrostatic energy, $\epsilon_{es}^{(10)}$, was found to clearly favor the T-shaped minimum ($\epsilon_{es}^{(10)} = -1580$ cm$^{-1}$) on the lowest A′ adiabat over the H-bonded Cl−H−Cl ($\epsilon_{es}^{(10)} = -400$ cm$^{-1}$) one.

Overall, the adiabatic surfaces provided by both approaches have many things in common. However, some quantitative differences exist which could be

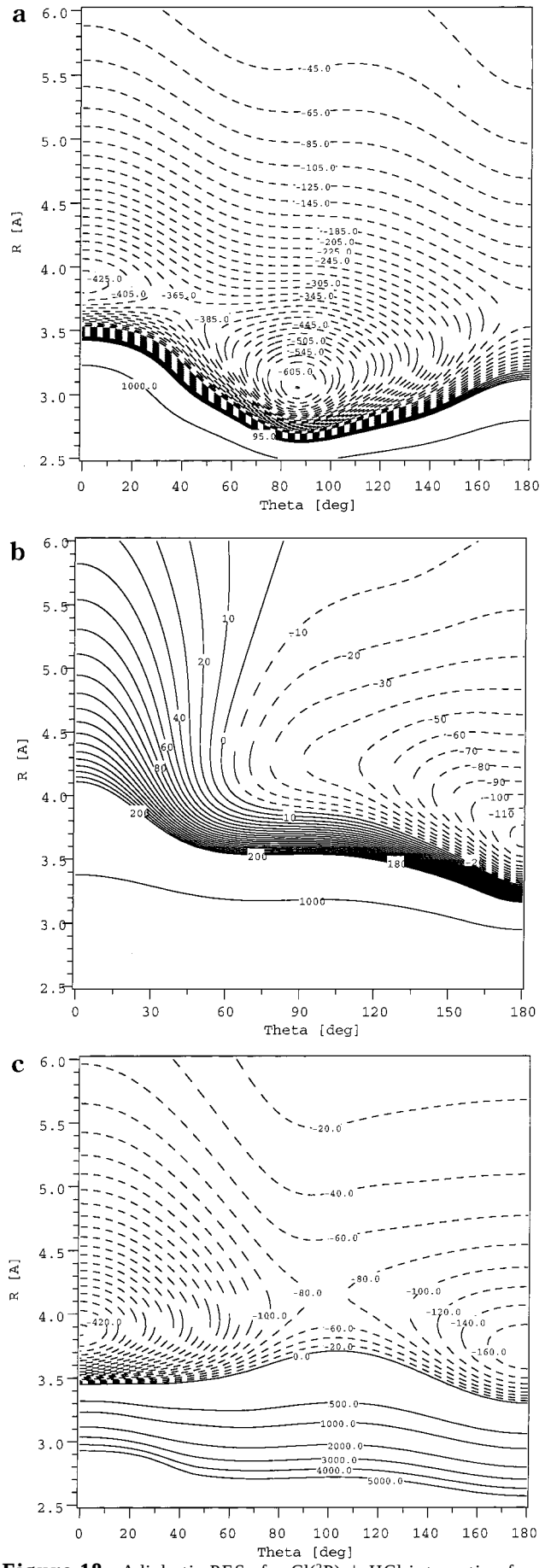


**Figure 18.** Adiabatic PESs for Cl($^2$P) + HCl interaction from ab initio calculations[168] (cm$^{-1}$): (a) $1^2A'$, (b) $2^2A'$, (c) $1^2A''$. $\Theta = 0°$ corresponds to the Cl−H−Cl hydrogen-bonded structure.

**Table 5. Characteristics of the Adiabatic PESs of Cl + HCl from ab Initio Calculations of Kłos et al.[168] and from Empirical Predictions of Dubernet and Hutson (D&H)[202]**

| state | reference | $R_e$ (Å) | $\Theta$ (°) | $D_e$ (cm$^{-1}$) |
|---|---|---|---|---|
| $1^2A'$ | Kłos et al.[168] | 3.05 | 86 | 625 |
| | | 3.85 | 0 | 442 |
| | D&H[202] | 3.6 | 90 | 347 |
| | | 3.9 | 0 | 383 |
| $2^2A'$ | Kłos et al.[168] | 3.7 | 180 | 128 |
| | D&H[202] | 4.2 | 150−180 | 50 |
| $1^2A''$ | Kłos et al.[168] | 3.85 | 0 | 442 |
| | | 3.7 | 180 | 174 |
| | D&H[202] | 3.9 | 0 | 383 |
| | | 3.7 | 180 | 200 |

sorted out in the future when the spectrum of this complex is observed. It is expected that these results will stimulate further experimental studies of Cl−HCl.

## *IV. Concluding Remarks*

Ab initio theory of van der Waals interactions has demonstrably evolved into a quantitative tool. As discussed in this review, the supermolecular approach based on the Møller−Plesset perturbation and coupled-cluster theories is capable of providing the rigorous, accurate, and physically meaningful description of intermolecular forces. Progress in computational resources enabled the routine use of sufficiently large basis sets, such as the correlation-consistent basis-set sequences. Modest improvements of these basis sets in the form of bond functions were shown to efficiently saturate the dispersion term. The use of highly correlated methods, such as CCSD(T), combined with large basis-set expansions are capable of providing accurate and complete intermolecular potential-energy surfaces. New computational methods, such as MP*n*-R12 and CCSD(T)-R12, allow for the simultaneous saturation of the basis-set and the correlation effects. We have demonstrated that the ab initio intermolecular PESs obtained following these strategies lead to predictions which are within experimental error bounds. With the advent of quantitative PESs, not only can the ab initio theory explain the experimental results, but also it can stimulate new experiments.

Despite this considerable progress, several fundamentally important questions remain. To explore larger clusters, it is necessary to include many-body interactions. Three-body interactions have been the subject of intense investigations in the past few years. The analysis of the individual nonadditive components of three-body effects in the range of clusters contributed greatly to our understanding of nonadditivity on the fundamental level and to the means of its accurate treatment. However, accurate three-body energies at the highest correlated level of theory are needed for many more systems. More insights into the analytical modeling of these terms should be gained. In particular, a modeling of exchange nonadditivity in the first and second order still lacks simple yet adequate functional templates. One cannot seriously think about simulations for clusters and bulk matter without solving this problem.

The studies of energy flow among the intra- and intermolecular vibrational modes and many other phenomena in state-to-state dynamics cannot be attempted without explicit inclusion of the intramolecular degrees of freedom in the potential surfaces. The construction of such PESs is a difficult task which can be simplified to a certain extent by the analysis of the energy components as functions of intramolecular geometries. We have pointed out in this review that highly correlated treatments are often needed even for qualitatively adequate description of intramonomer vibration and relaxation. More work in this direction is warranted.

van der Waals complexes with the open-shell moieties are considerably more complex, because their interactions are often characterized by multiple, closely spaced potential surfaces. Significant progress in the treatment of such van der Waals clusters has been achieved in recent years due in large measure to the studies of the RG−open-shell atom/molecule complexes which can serve as valuable nonreactive models for a number of elementary reactions. van der Waals complexes are often formed in well regions in reactant valleys of chemical reactions. The studies of the role of these complexes in the reaction dynamics have barely begun. In ab initio calculations of the complete reactive surfaces, one has to reconcile the different computational needs of the reactive vs the prereactive regions of the PES. The currently used methods are tuned to the demands of either one or the other. As techniques such as multireference coupled cluster become more developed, the reactive surfaces could, hopefully, be calculated in a more routine fashion. Nevertheless, some notable successes have already been achieved in ab initio PESs which model reliably both the reactive and prereactive regions. For example, the highly accurate PES for the reaction $F + H_2 \rightarrow FH + H$ assembled by Stark and Werner[100] served as a watershed event for both theory and experiment.[203] Ab initio calculations have already provided valuable insights into harpooning reactions, Na−FH[173] and Ca−ClH,[204] and many other types of reactions, e.g., refs 101 and 200. The quantitative nature of these calculations enabled a particularly synergistic interplay between theory and experiment. The recent flurry of activity includes studies of spin−orbit coupling and nonadiabatic reaction channels. A full understanding of multisurface dynamics will continue to demand further theoretical and experimental effort.

## V. Abbreviations

| | |
|---|---|
| AIM | relativistic atoms-in-molecule approach |
| ACPF | average coupled pair functional |
| BSSE | basis-set superposition error |
| CASSCF | complete active space |
| CASPT2/3 | complete active space perturbation theory (second/third order) |
| CBS | complete basis set |
| CC | coupled-cluster theory |
| CCSD | coupled-cluster theory with singles and doubles |
| CCSD(T) | coupled-cluster theory with singles, doubles, and noniterative triples |
| CCSD(T)-R12 | coupled-cluster theory with singles, doubles, and noniterative triples with explicit inclusion of linear $r_{12}$ terms |
| CEPA | coupled electron pair approximation |
| CHA | chemical Hamiltonian approach |
| CI | configuration interaction |
| CP | counterpoise |
| DCBS | dimer-centered basis set |
| DFT | density functional theory |
| GVB | general valence bond |
| HF | Hartree−Fock |
| HL | Heitler−London |
| MC | Monte Carlo |
| MP | Møller−Plesset perturbation theory, many-body perturbation theory |
| MP2 | Møller−Plesset perturbation theory through the second order |
| MP2−R12 | second-order Møller−Plesset theory with explicit inclusion of linear $r_{12}$ terms |
| MP*n*-R12 | *n*th-order Møller−Plesset theory with explicit inclusion of linear $r_{12}$ terms |
| MP3 | Møller−Plesset perturbation theory through the third order |
| MP4 | Møller−Plesset perturbation theory through the fourth order |
| MP5 | Møller−Plesset perturbation theory through the fifth order |
| MRCI | multireference configuration interaction |
| LMP2 | local-correlation Møller−Plesset perturbation theory through the second order |
| LMP4(SDQ) | local-correlation fourth-order Møller−Plesset with singles, doubles, and quadruples |
| LCCSD | local-correlation coupled-cluster theory with singles and doubles |
| PES | potential-energy surface |
| RCCSD(T) | partially spin-restricted coupled cluster with singles, doubles, and noniterative triples |
| RG | rare gas |
| RS | Rayleigh−Schroedinger |
| SAPT | symmetry-adapted perturbation theory |
| SE | single exchanges |
| SEP | stimulated-emission pumping |
| SCF | self-consistent field |
| S-MP | supermolecular Møller−Plesset perturbation theory |
| TE | triple exchanges |
| UCCSD(T) | unrestricted coupled cluster with singles, doubles, and noniterative triples |
| UHF | unrestricted Hartree−Fock theory |
| UMP | unrestricted Møller−Plesset perturbation theory |
| UMP4 | unrestricted Møller−Plesset theory through the fourth order |
| VRT | vibration−rotation−tunneling spectroscopy |

## VI. Acknowledgments

Many results described in this review represent a group effort of many collaborators. We thank J. Kłos, S. M. Cybulski, R. Burcl, A. A. Buchachenko, M. W. Severson, J. Jakowski, R. Bukowski, R. A. Kendall, and M. Gutowski for their contributions. We are especially grateful to Bogumil Jeziorski for offering us his comments on this manuscript. This work was supported by the National Science Foundation (CHE-9527099) and by the Polish Committee for Scientific Research (Grant No. 3 T09A 112 18).

## VII. References


(1) van der Waals Molecules II. *Chem. Rev.* **1994**, *94*, entire issue.
(2) Chałasiński, G.; Szczęśniak, M. M. *Chem. Rev.* **1994**, *94*, 1723.
(3) Jeziorski, B.; Moszynski, R.; Szalewicz, K. *Chem. Rev.* **1994**, *94*, 1887.
(4) van Duijneveldt, F.; van Duijneveldt-van de Rijdt, G. C. J. M.; van Lenthe, J. H. *Chem. Rev.* **1994**, *94*, 1873.
(5) van der Avoird, A.; Wormer, P. E. S.; Moszynski, R. *Chem. Rev.* **1994**, *94*, 1931.
(6) *Molecular Interactions from van der Waals to Strongly Bound*; Scheiner, S., Ed.; Wiley: Chichester, 1997.
(7) *Theoretical Treatments of Hydrogen Bonding*; Hadži, D., Ed.; Wiley: Chichester, 1997.
(8) Chałasiński, G.; Kłos, J.; Cybulski, S. M.; Szczęśniak, M. M. *Collect. Czech. Chem. Commun.* **1998**, *63*, 1473.
(9) Skouteris, D.; Manolopoulos, D. E.; Bian, W.; Werner, H.-J.; Lai, L.-H., Liu, K. *Science* **1999**, *286*, 1713.
(10) Alexander, M. H. *J. Chem. Phys.* **1998**, *108*, 4467.
(11) Buchachenko A. A.; Jakowski, J.; Chałasiński, G.; Szczęśniak, M. M.; Cybulski, S. M. *J. Chem. Phys.* **2000**, *112*, 5852.
(12) Alexander, M. H.; Werner, J.-H., Manolopoulos, D. E. *J. Chem. Phys.* **1998**, *109*, 5710.
(13) Rak, J.; Szczęśniak, M. M.; Chałasiński, G.; Cybulski, S. M. *Pol. J. Chem.* **1998**, *72*, 1505.
(14) Jeziorski, B.; Szalewicz, K. In *The Encyclopedia of Computational Chemistry*;, von Rague Schleyer, P., Allinger, N. L., Clark, T., Gasteiger, J., Kollman, P. A., Schaefer, H. F., III., Schreiner, R., Eds.; Wiley: Chichester, UK, 1988; Vol. 4, p 1376. Jeziorski, B.; Szalewicz, K. *J. Chem. Phys.* **1998**, *109*, 1198.
(15) Boys, S. F.; Bernardi, F. *Mol. Phys.* **1970**, *19*, 553.
(16) van Lenthe, J. H.; van Duijneveldt-van de Rijdt, J. G. C. M.; van Duijneveldt, F. B. *Adv. Chem. Phys.* **1987**, *69*, 521.
(17) Xantheas, S. S. *J. Chem. Phys.* **1996**, *104*, 8821.
(18) Simon, S.; Duran, M.; Dannenberg, J. J. *J. Chem. Phys.* **1996**, *105*, 11024.
(19) Hobza, P.; Bludsky, O.; Suhai, S. *Phys. Chem. Chem. Phys.* **1999**, *1*, 3073.
(20) Morokuma, K. *J. Chem. Phys.* **1971**, *55*, 1236.
(21) Szczęśniak, M. M.; Chałasiński, G. In *Molecular Interactions from van der Waals to Strongly Bound*; Scheiner, S., Ed.; Wiley: Chichester, 1997; p 45.
(22) Kłos, J.; Chałasiński, G.; Berry, M. T.; Kendall, R. A.; Burcl, R.; Szczęśniak, M. M.; Cybulski, S. M. *J. Chem. Phys.* **2000**, *112*, 4952.
(23) Halkier, A.; Klopper, W.; Helgaker, T.; Jørgensen, P.; Taylor, P. R. *J. Chem. Phys.* **1999**, *111*, 9157.
(24) Klopper, W.; Quack, M.; Suhm, M. A. *J. Chem. Phys.* **1998**, *108*, 10096.
(25) Olsen, J.; Christiansen, O.; Koch, H.; Jørgensen, P. *J. Chem. Phys.* **1996**, *105*, 5082. Olsen, J.; Jørgensen, P.; Helgaker, T.; Christiansen, O. *J. Chem. Phys.* **2000**, *112*, 9736. Stillinger, F. H. *J. Chem. Phys.* **2000**, *112*, 9711. Leininger, M. L.; Allen, W. D.; Schaefer, H. F., III; Sherrill, C. D. *J. Chem. Phys.* **2000**, *112*, 9213.
(26) Rohrbacher, A.; Williams, J.; Janda, K. C.; Cybulski, S. M.; Burcl, R.; Szczęśniak, M. M.; Chałasiński, G.; Halberstadt, N. *J. Chem. Phys.* **1997**, *106*, 2685.
(27) Rak, J.; Szczęśniak, M. M.; Chałasiński, G.; Cybulski, S. M. *J. Chem. Phys.* **1997**, *106*, 10215.
(28) Kłos, J.; Chałasiński, G.; Berry, M. T.; Bukowski, R.; Cybulski, S. M. *J. Chem. Phys.* **2000**, *112*, 2195.
(29) Rode, M.; Sadlej, J.; Moszynski, R.; Wormer, P. E. S.; van der Avoird, A. *Chem. Phys. Lett.* **1999**, *314*, 326.
(30) Jeziorski, B.; Moszynski, R.; Ratkiewicz, A.; Rybak, S.; Szalewicz, K.; Williams, H. L. SAPT: A Program for Many-Body Symmetry-Adapted Perturbation Theory Calculations of Intermolecular Interaction Energies. In *Methods and Techniques in Computational Chemistry: METECC-94*; Clementi, E., Ed.; STEF: Gagliari, 1993; Vol. B.
(31) Adams, W. H. *Int. J. Quantum Chem.* **1996**, *60*, 273 and references therein.
(32) Mas, E. M.; Szalewicz, K.; Bukowski, R.; Jeziorski, B. *J. Chem. Phys.* **1997**, *107*, 4207.
(33) Moszynski, R.; Heijmen, T. G. A.; Jeziorski, B. *Mol. Phys.* **1996**, *88*, 741.
(34) Moszynski, R.; Wormer, P. E. S.; Heijmen, T. G. A.; van der Avoird *J. Chem. Phys.* **1998**, *108*, 579.
(35) Chałasiński, G.; Rak, J.; Szczęśniak, M. M.; Cybulski, S. M. *J. Chem. Phys.* **1997**, *106*, 3301
(36) Guo, H.; Sirois, S.; Proynov, E. I.; Salahub, D. R. In *Theoretical Treatments of Hydrogen Bonding*; Hadži, D., Ed.; Wiley: Chichester, 1997; p 49.
(37) Mok, D. K. W.; Handy, N. C.; Amos, R. D. *Mol. Phys.* **1997**, *92*, 667.
(38) Zaremba, E.; Kohn, W. *Phys. Rev.* **1976**, *B13*, 2278; **1977**, *B15*, 1769.
(39) Milet, A.; Korona, T.; Moszynski, R.; Kochanski, E. *J. Chem. Phys.* **1999**, *111*, 7727.
(40) Gianturco, F. A.; Lewerenz, M.; Paesani, F.; Toennies, J. P. *J. Chem. Phys.* **2000**, *112*, 2239. Gianturco, F. A.; Paesani, F.; Laranjeira, M. F.; Vassilenko, V.; Cunha, M. A. *J. Chem. Phys.* **2000**, *112* 7832.
(41) Saebo, S.; Pulay, P. *J. Chem. Phys.* **1987**, *86*, 914.
(42) Saebo, S.; Pulay, P. *Annu. Rev. Phys. Chem.* **1993**, *44*, 213.
(43) Saebo, S.; Tong, W.; Pulay, P. *J. Chem. Phys.* **1993**, *98*, 2170.
(44) Schutz, M.; Rauhut, G.; Werner, H.-J. *J. Phys. Chem. A* **1998**, *102*, 5997.
(45) Runeberg, N.; Schutz, M.; Werner, H.-J. *J. Chem. Phys.* **1999**, *110*, 7210.
(46) Chałasiński, G.; Szczęśniak, M. M. *Mol. Phys.* **1988**, *63*, 205.
(47) Hetzer, G.; Pulay, P.; Werner, H.-J. *Chem. Phys. Lett*, **1998**, *290*, 143.
(48) Hampel, C.; Werner, H.-J. *J. Chem. Phys.* **1996**, *104*, 6286.
(49) Taylor, P. R. in: *Lecture Notes in Quantum Chemistry*; Roos, B. O., Ed.; Springer-Verlag: New York, 1992; p 325.
(50) (a) Liedl, K. R. *J. Chem. Phys.* **1998**, *108*, 3199. (b) Tarakeshwar, P.; Choi, H. S.; Lee, J. S.; Kim, K. S.; Ha, T.-K.; Jang, J. H.; Lee, J. G.; Lee, H. *J. Chem. Phys.* **1999**, *111*, 5838.
(51) Salvador, P.; Paizs, B.; Duran, M.; Suhai, S. Manuscript in preparation.
(52) Gutowski, M.; Szczęśniak, M. M.; Chałasiński, G. *Chem. Phys. Lett.* **1995**, *241*, 140.
(53) Cybulski, S. M.; Chałasiński, G. *Chem. Phys. Lett.* **1992**, *197*, 591.
(54) Szczęśniak, M. M.; Scheiner, S. *J. Chem. Phys.* **1986**, *84*, 6328.
(55) Gutowski M.; Chałasiński, G. *J. Chem. Phys.* **1993**, *98*, 5540.
(56) Gutowski, M.; van Duijneveldt-van de Rijdt, J. G. C. M.; van Lenthe, J. H.; van Duijneveldt, F. B. *J. Chem. Phys.* **1993**, *98*, 4728.
(57) van Duijneveldt, F. B. In *Molecular Interactions from van der Waals to Strongly Bound*; Scheiner, S., Ed.; Wiley: Chichester, 1997; p 81.
(58) Mayer, I.; Valiron, P. *J. Chem. Phys.* **1998**, *109*, 3360.
(59) Kutzelnigg, W. *Theor. Chim. Acta* **1985**, *68*, 445.
(60) Klopper, W. *The Encyclopedia of Computational Chemistry*; von Rague Schleyer, P., Allinger, N. L., Clark, T., Gasteiger, J., Kollman, P. A., Schaefer, H. F., III., Schreiner, R., Eds.; Wiley: Chichester, UK, 1988; Vol. 4, p 2351
(61) Burcl, R.; Chałasiński, G.; Bukowski, R.; Szczęśniak, M. M. *J. Chem. Phys.* **1995**, *103*, 1498.
(62) Jeziorski, B.; Szalewicz, K.; Monkhorst, H., Zabolitzky, J. G. *J. Chem. Phys.* **1984**, *81*, 368.
(63) Bukowski, R.; Jeziorski, B.; Rybak, S.; Szalewicz, K. *J. Chem. Phys.* **1995**, *102*, 888.
(64) Bukowski, R.; Jeziorski, B.; Szalewicz, K. *J. Chem. Phys.* **1996**, *104*, 3306.
(65) Korona, T.; Williams, H. L.; Bukowski, R.; Jeziorski, B.; Szalewicz, K. *J. Chem. Phys.* **1997**, *106*, 5109.
(66) Klopper, W. *J. Chem. Phys.* **1995**, *102*, 6168.
(67) Klopper, W.; Schütz, M.; Lüthi, H. P.; Leutwyler, S. *J. Chem. Phys.* **1995**, *103*, 1.
(68) Klopper, W.; Quack, M.; Suhm, M. A. *Mol. Phys.* **1998**, *94*. 105.
(69) Tao, F.-M.; Pan, Y.-K. *J. Chem. Phys.* **1992**, *97*, 4989.
(70) Koch, H.; Fernandez, B.; Christiansen, O. *J. Chem. Phys.* **1998**, *108*, 2784.
(71) Cybulski, S. M.; Toczyłowski, R. *J. Chem. Phys.* **1999**, *111*, 10520.
(72) (a) van Mourik, T.; Wilson, A. K.; Dunning, T. H. *Mol. Phys.* **1999**, *96*, 529. (b) Aziz, R. A. *J. Chem. Phys.* **1993**, *99*, 4518.
(73) van Duijneveldt-van de Rijdt, J. G. C. M.; van Duijneveldt, F. B. In *Theoretical Treatments of Hydrogen Bonding*; Hadži, D., Ed.; Wiley: Chichester, 1997; p 13.
(74) Sadlej, A. J. *Collect. Czech. Chem. Commun.* **1988**, *53*, 1995. Sadlej, A. J. *Theor. Chim. Acta* **1991**, *79*, 123. Sadlej, A. J.; Urban, J. *J. Mol. Struct. (THEOCHEM)* **1991**, *234*, 147. Sadlej, A. J.; Urban, J. *Theor. Chim. Acta* **1991**, *81*, 45. Sadlej, A. J.; Urban *Theor. Chim. Acta* **1992**, *81*, 339. Kello, V.; Sadlej, A. J. *Theor. Chim. Acta* **1992**, *83*, 351. Miadokov, I.; Kello, V.; Sadlej, A. J. *Theor. Chem. Acc.* **1997**, *96*, 166.
(75) van Duijneveldt-van de Rijdt, J. G. C. M.; van Duijneveldt, F. B. *J. Chem. Phys.* **1999**, *111*, 3812.
(76) Dunning, T. H., Jr. *J. Chem. Phys.* **1989**, *90*, 1007. Kendall, R. A.; Dunning, T. H., Jr.; Harrison, R. J. *J. Chem. Phys.* **1992**, *96*, 6796. Woon, D. E.; Dunning, T. H., Jr. *J. Chem. Phys.* **1993**, *98*, 1358.
(77) van Mourik, T.; Dunning, T. H. *J. Chem. Phys.* **1999**, *111*, 9248.
(78) Woon, E. D.; Peterson, K. A.; Dunning, T. H. *J. Chem. Phys.* **1998**, *109*, 2233.
(79) van Mourik, T.; Dunning, T. H. *J. Chem. Phys.* **1997**, *107*, 2451.
(80) Feyereisen, M. W.; Feller, D.; Dixon, D. A. *J. Phys. Chem.* **1996**, *100*, 2993. Peterson, K. A.; Dunning, T. H. *J. Chem. Phys.* **1995**, *102*, 2032.
(81) McBane, G. C.; Cybulski, S. M. *J. Chem. Phys.* **1999**, *110*, 11734.
(82) Antonova, S.; Lin, A.; Tsakotellis, A. P.; McBane, G. C. *J. Chem. Phys.* **1999**, *110*, 11742.

(83) Moszynski, R.; Korona, T.; Wormer, P. E. S.; van der Avoird, A. *J. Phys. Chem.* **1997**, *101*, 4690.
(84) Moszynski, R.; Wormer, P. E. S.; Jeziorski, B.; van der Avoird, A. *J. Chem. Phys.* **1994**, *101*, 4690. Moszynski, R.; Jeziorski, B.; van der Avoird, A.; Wormer, P. E. S. *J. Chem. Phys.* 2825.
(85) Heijmen, T.; Moszynski, R.; Wormer, P. E. S.; van der Avoird, A. *J. Chem. Phys.* **1997**, *107*, 9921.
(86) Koch, H.; Fernandez, B.; Makarewicz, J. *J. Chem. Phys.* **1999**, *111*, 198.
(87) Fernandez, B.; Koch, H.; Makarewicz, J. *J. Chem. Phys.* **1999**, *110*, 8525.
(88) Cohen R. C.; Saykally, R. J. *Annu. Rev. Phys. Chem.* **1991**, *42*, 369.
(89) LeRoy, R. J.; Hutson, J. M. *J. Chem. Phys.* **1987**, *86*, 837.
(90) Hutson, J. M. *J. Chem. Phys.* **1992**, *96*, 6752.
(91) Bader, R. F. *Atoms in Molecules*; Clarendon Press: Oxford, 1994.
(92) Chuang, C. C.; Higgins, K. J.; Fu, H. C.; Klemperer, W. *J. Chem. Phys.* **2000**, *112*, 7022.
(93) Jeziorska, M.; Jankowski, P.; Szalewicz, K.; Jeziorski, B. *J. Chem. Phys.* **2000**, *113*, 2957.
(94) Chang, H. C.; Tao, F. M.; Klemperer, W.; Healey, C.; Hutson, J. M. *J. Chem. Phys.* **1993**, *99*, 9337.
(95) Naumkin, F. Y.; Knowles, P. J. *J. Chem. Phys.* **1995**, *103*, 3392.
(96) Williams, J.; Rohrbacher, A.; Seong, J.; Maranayagam, N.; Janda, K. C.; Burcl, R.; Szczęśniak, M. M.; Chałasiński, G.; Cybulski, S. M.; Halberstadt, N. *J. Chem. Phys.* **1999**, *111*, 997.
(97) Naumkin, F. Y.; McCourt, F. R. W. *J. Chem. Phys.* **1998**, *108*, 9301.
(98) Naumkin, F. Y. *J. Chem. Phys.* **1997**, *107*, 5702.
(99) Bartlett, R. J. In Modern Electronic Structure Theory, Part II; Yarkony, D. R., Ed.; World Scientific: Singapore 1995; p 1047. Bartlett, R. J.; Stanton, J. F. Applications of Post-Hartree−Fock Methods: A Tutorial. In *Reviews in Computational Chemistry*; Lipkowitz, K. B., Boyd, D. B. Eds.; VCH Publishers: New York, 1994; Vol. V.
(100) Stark, K.; Werner, H.-J. *J. Chem. Phys.* **1996**, *104*, 6515.
(101) Bian, W.; Werner, H.-J. *J. Chem. Phys.* **2000**, *112*, 220.
(102) Quack, M.; Suhm, M. A. *J. Chem. Phys.* **1991**, *95*, 28.
(103) Bunker, P. R.; Epa, E. V.; Jensen, P.; Karpfen, A. *J. Mol. Spectrosc.* **1991**, *146*, 200.
(104) Karpfen, A.; Bunker, P. R.; Jensen, P. *Chem. Phys.* **1991**, *149*, 299.
(105) Wu, Q.; Zhang, D. H.; Zhang, J. Z. H. *J. Chem. Phys.* **1995**, *103*, 2548.
(106) Zhang, D.; Wu, Q.; Zhang, J. Z. H.; von Dirke, M.; Bacič, Z. *J. Chem. Phys.* **1995**, *102*, 2315.
(107) Elrod, M. J.; Saykally, R. J. *J. Chem. Phys.* **1995**, *103*, 933.
(108) Qiu, Y.; Bacič, Z. *J. Chem. Phys.* **1996**, *106*, 2158.
(109) Qiu, Y.; Zhang, J. Z. H.; Bacič, Z. *J. Chem. Phys.* **1998**, *108*, 4804.
(110) Millot, C.; Stone, A. J. *Mol. Phys.* **1992**, *77*, 439.
(111) Groenenboom, G. C.; Mas, E. M.; Bukowski, R.; Szalewicz, K.; Wormer, P. E. S.; van der Avoird, A. *Phys. Rev. Lett.* **2000**, *84*, 4072.
(112) Moszynski, R.; Wormer, P. E. S.; Jeziorski, B.; van der Avoird, A. *J. Chem. Phys.* **1995**, *103*, 8085; *J. Chem. Phys.* **1997**, *107*, E672.
(113) Lotrich, V.; Szalewicz, K.; *J. Chem. Phys.* **1997**, *106*, 9668.
(114) Lotrich, V. F.; Jankowski, P.; Szalewicz, K. *J. Chem. Phys.* **1998**, *108*, 4725.
(115) Szczęśniak, M. M.; Chałasiński, G. *J. Mol. Struct. (THEOCHEM)* **1992**, *261*, 37.
(116) Turki, N.; Milet, A.; Rahamouni, A.; Ouamerali, O.; Moszynski, R.; Kochanski, E.; Wormer, P. E. S. *J. Chem. Phys.* **1998**, *109*, 7157.
(117) Milet, A.; Moszynski, R.; Wormer, P.; van der Avoird *J. Phys. Chem.* **A 1999**, *103*, 6811.
(118) Xantheas, S. S. *J. Chem. Phys.* **1994**, *100*, 7523.
(119) Clementi, E.; Kołos, W.; Lie, G. C.; Ranghino, G. *Int. J. Quantum Chem.* **1980**, *17*, 377.
(120) Chałasiński, G.; Szczęśniak, M. M.; Cieplak, P.; Scheiner, S. *J. Chem. Phys.* **1991**, *94*, 2873.
(121) Szczęśniak, M. M.; Chałasiński, G.; Cybulski, S. M.; Scheiner, S. *J. Chem. Phys.* **1990**, *93*, 4243.
(122) Chałasiński, G.; Szczęśniak, M. M.; Kendall, R. A. *J. Chem. Phys.* **1994**, *101*, 8860.
(123) Szczęśniak, M. M.; Chałasiński, G.; Piecuch, P. *J. Chem. Phys.* **1993**, *99*, 6732.
(124) Cybulski, S. M.; Szczęśniak, M. M.; Chałasiński, G. *J. Chem. Phys.* **1994**, *101*, 10708.
(125) Jansen, L. *Adv. Quantum Chem.* **1965**, *2*, 119
(126) Cooper, A. R.; Hutson, J. M. *J. Chem. Phys.* **1993**, *98*, 5337.
(127) Lotrich, V. F.; Szalewicz, K.; Jeziorski, B. *Pol. J. Chem.* **1998**, *72*, 1826
(128) Hasse, R.; Severson, M.; Szczęśniak, M. M.; Chałasiński, G.; Cieplak, P.; Kendall, R. A.; Cybulski, S. M. *J. Mol. Struct.* **1997**, *436−437*, 387.
(129) Kukawska-Tarnawska, B.; Chałasiński, G.; Szczęśniak, M. M. *J. Chem. Phys.* **1996**, *105*, 8213.
(130) Jakowski, J.; Chałasiński, G.; Szczęśniak, M. M.; Cybulski, S. M. *Chem. Phys. Phys. Lett.* **1998**, *239*, 573.
(131) Elrod, M. J.; Saykally, R. J.; Cooper, A. R.; Hutson, J. M. *Mol. Phys.* **1994**, *81*, 579.
(132) Ernesti, A.; Hutson, J. M. *Faraday Discuss. Chem. Soc.* **1994**, *97*, 119
(133) Ernesti, A.; Hutson, J. M. *Phys. Rev. A* **1995**, *51*, 239.
(134) Ernesti, A.; Hutson, J. M. *J. Chem. Phys.* **1997**, *106*, 6288.
(135) McIlroy, A.; Lascola, R.; Lovejoy, C. M.; Nesbitt, D. J. *J. Phys. Chem.* **1991**, *95*, 2636.
(136) Hutson, J. M.; Liu, S.; Moskowitz, J. W.; Bacič Z. *J. Chem. Phys.* **1999**, *111*, 8378.
(137) Chuang, C.-C.; Tsang, N. S.; Hanson, J. G.; Klemperer, W.; Chang, H.-C. *J. Chem. Phys.* **1997**, *107*, 7041.
(138) Kłos, J.; Szczęśniak, M. M.; Chałasiński, G. Manuscript in preparation.
(139) Lotrich, V. F.; Szalewicz, K. *J. Chem. Phys.* **2000**, *112*, 112.
(140) Wormer, P. E. S.; Moszynski, R.; van der Avoird, A. *J. Chem. Phys.* **2000**, *112*, 3159.
(141) Chałasiński, G.; Szczęśniak, M. M.; Scheiner, S. *J. Chem. Phys.* **1991**, *94*, 2807.
(142) Arunan, E.; Emilsson, T.; Gutowsky, H. S. *J. Am. Chem. Soc.* **1994**, *116*, 8418.
(143) Arunan, E.; Dykstra, C. E.; Emilsson, T.; Gutowsky, H. S. *J. Chem. Phys.* **1996**, *105*, 8495.
(144) Liu, S.; Bacič, Z.; Moskowitz, J. W.; Schmidt, K. E. *J. Chem. Phys.* **1994**, *101*, 8310.
(145) Burcl, R., Ph.D. Dissertation, Oakland University, Rochester, 1999.
(146) Burcl, R.; Szczęśniak, M. M.; Kłos, J.; Chałasiński, G.; Cybulski, S. M. Manuscript in preparation.
(147) Sperhac, J. M.; Weida, M. J.; Nesbitt, D. J. *J. Chem. Phys.* **1996**, *104*, 2202.
(148) Burcl, R.; Cybulski, S. M.; Szczęśniak, M. M.; Chałasiński, G. *J. Chem. Phys.* **1995**, *103*, 299.
(149) Yourshaw, I.; Zhao, Y.; Neumark, D. M. *J. Chem. Phys.* **1996**, *105*, 351.
(150) Heaven, M. C. *Annu. Rev. Phys. Chem.* **1992**, *43*, 283; *J. Phys. Chem.* **1993**, *97*, 8567.
(151) Dubernet, M. L.; Hutson, J. M. *J. Chem. Phys.* **1994**, *101*, 1939.
(152) Polanyi, J. C. *Acc. Chem. Res.* **1972**, *5*, 161.
(153) Sinha, A.; Thoemke, J. D.; Crimm, F. F. *J. Chem. Phys.* **1992**, *96*, 372.
(154) Anderson, D. T.; Schwartz, R. L.; Todd, M. W.; Lester, M. I. *J. Chem. Phys.* **1998**, *109*, 3461.
(155) Aquilanti, V.; Liuti, G.; Pirani, F.; Vecchiocattivi, F. *J. Chem. Soc., Faraday Trans. 2* **1989**, *85*, 955.
(156) Yarkony, D. R. *J. Phys. Chem.* **1996**, *100*, 18612.
(157) Cybulski, S. M.; Kendall, R. A.; Chałasiński, G.; Severson, M. W.; Szczęśniak, M. M. *J. Chem. Phys.* **1997**, *106*, 7731.
(158) Kendall, R. A.; Chałasiński, G.; Kłos, J.; Bukowski, R.; Severson, M. W.; Szczęśniak, M. M.; Cybulski, S. M. *J. Chem. Phys.* **1998**, *108*, 3235.
(159) Cybulski, S. M.; Chałasiński, G.; Szczęśniak, M. M. *J. Chem. Phys.* **1996**, *105*, 9525.
(160) Burcl, R.; Krems, R. V.; Buchachenko, A. A.; Szczęśniak, M. M.; Chałasiński, G.; Cybulski, S. M. *J. Chem. Phys.* **1998**, *109*, 2144.
(161) Buchachenko, A. A.; Krems, R. V.; Xiao, Y. D.; Szczęśniak, M. M.; Chałasiński, G.; Viehland, L. A. Manuscript in preparation.
(162) Alexander, M. H. *J. Chem. Phys.* **1999**, *111*, 7426.
(163) Alexander, M. H. *J. Chem. Phys.* **1993**, *99*, 6014.
(164) Cybulski, S. M.; Chałasiński, G.; Szczęśniak, M. M. *J. Chem. Phys.* **1996**, *105*, 9525.
(165) Mead, C. A.; Truhlar, D. G. *J. Chem. Phys.* **1982**, *77*, 6090.
(166) Rebentrost, F.; Lester, W. A., Jr. *J. Chem. Phys.* **1975**, *63*, 3737.
(167) Werner, H. J.; Follmeg, B.; Alexander, M. H. *J. Chem. Phys.* **1988**, *89*, 3139.
(168) Kłos, J.; Chałasiński, G.; Szczęśniak, M. M. Manuscript in preparation.
(169) Kłos, J.; Chałasiński, G.; Szczęśniak, M. M. Manuscript in preparation.
(170) van Lenthe, J. H.; van Dam, T.; van Duijneveldt, F. B.; Kroon-Batenburg, L. M. J. *Faraday Symp. Soc.* **1984**, *19*, 1.
(171) Vos, R. J.; van Lenthe, J. H.; van Duijneveldt, F. B. *J. Chem. Phys.* **1990**, *93*, 643.
(172) van Mourik, T., Ph.D. Dissertation, University of Utrecht, 1994.
(173) Topaler, M. S.; Truhlar, D. G.; Chang, X. Y.; Piecuch, P.; Polanyi, J. C. *J. Chem. Phys.* **1998**, *108*, 5349.
(174) Kaledin, A. L.; Heaven, M. C.; Lawerence, W. G.; Cui, Q.; Stevens, J. E.; Morokuma, K. *J. Chem. Phys.* **1998**, *108*, 2771.
(175) Wayne, R. P. *Chemistry of Athmospheres: An Introduction to the Chemistry of the Atmospheres of Earth, the Planets, and their Satellites*; Oxford University Press: Oxford, 1991.
(176) Berry, M. T.; Brustein, M. R.; Lester, M. I.; Chakravarty, C.; Clary, D. C. *Chem. Phys. Lett.* **1991**, *178*, 301.
(177) Berry, M. T.; Loomis, R. A.; Giancarlo, L. C.; Lester, M. I. *J. Chem. Phys.* **1992**, *96*, 7890.

(178) Lester, M. I.; Green, W. H., Jr.; Chakravarty, C.; Clary, D. C. In *Molecular Dynamics and Spectroscopy by Stimulated Emission Pumping*; Dai, H. L., Field, R. W., Eds.; World Scientific: 1995; p 659.
(179) Dubernet, M. L.; Hutson, J. M. *J. Chem. Phys.* **1993**, *99*, 7477.
(180) Degli Esposti, A.; Werner, H.-J. *J. Chem. Phys.* **1990**, *93*, 3351.
(181) Degli Esposti, A.; Berning, A.; Werner, H.-J. *J. Chem. Phys.* **1995**, *103*, 2067.
(182) Fawzy, W. M.; Heaven, M. C. *J. Chem. Phys.* **1990**, *92*, 909.
(183) Chang, B.-C.; Yu, L.; Cullin, D.; Refuss, B.; Williamson, J.; Miller, T. A.; Fawzy, W. M.; Zheng, X.; Fei, S.; Heaven, M. C. *J. Chem. Phys.* **1991**, *95*, 7086.
(184) Oshima, Y.; Iida, M.; Endo, Y. *J. Chem. Phys.* **1991**, *95*, 7001.
(185) Chakravarty, C.; Clary, D. C. *J. Chem. Phys.* **1991**, *94*, 4149.
(186) Chakravarty, C.; Clary, D. C. Esposti, A. D.; Werner, H.-J. *J. Chem. Phys.* **1990**, *93*, 3367.
(187) Chakravarty, C.; Clary, D. C. *Chem Phys Lett* **1990**, *173*, 541.
(188) Bonn, R. T.; Wheeler, M. D.; Lester, M. I. *J. Chem. Phys.* **2000**, *112*, 4942.
(189) (a) van Beek, M. C.; ter Meulen, J. J.; Alexander, M. H. *J. Chem. Phys.* **2000**, *113*, 628. (b) van Beek, M. C.; ter Meulen, J. J.; Alexander, M. H. *J. Chem. Phys.* **2000**, *113*, 637.
(190) Alexander, M. H.; Gregurick, S.; Dagdigian, P. J.; Lemire, G. W.; McQuaid, M. J.; Sausa, R. C. *J. Chem. Phys.* **1994**, *101*, 4547.
(191) Wagner, A. F.; Dunning, T. H., Jr; Kok, R. *J. Chem. Phys.* **1994**, *100*, 1326.
(192) Basinger, W. H.; Lawrence, W. H.; Heaven, M. C. *J. Chem. Phys.* **1995**, *103*, 7218.
(193) Alexander, M. H.; Kearney, W. H.; Wagner, A. F. *J. Chem. Phys.* **1994**, *100*, 1338.
(194) Kukawska-Tarnawska, B.; Chałasiński, G.; Olszewski, K. *J. Chem. Phys.* **1994**, *101*, 4964.
(195) Cybulski, S. M.; Burcl, R.; Chałasiński, G.; Szczęśniak, M. M. *J. Chem. Phys.* **1995**, *103*, 10116.
(196) Cybulski, S. M.; Burcl, R.; Chałasiński, G.; Szczęśniak, M. M. *J. Chem. Phys.* **1996**, *104*, 7997.
(197) Bililign, S.; Gutowski, M.; Simons, J.; Breckenridge, W. H. *J. Chem. Phys.* **1994**, *100*, 8212.
(198) Arnold, S. T.; Hendricks, J. H.; Bowen, K. H. *J. Chem. Phys.* **1995**, *102*, 39.
(199) deClercq, H. L.; Hendricks, J. H.; Bowen, K. H. Manuscript in preparation.
(200) Dobbyn, A. J.; Connor, J. N. I.; Besley, N. A.; Knowles, P. J.; Schatz, G. C. *Phys. Chem. Chem. Phys.* **1999**, *1*, 957.
(201) Liu, K.; Kolessov, A.; Partin, J. W.; Benzel, I.; Wittig, C. *Chem. Phys. Lett.* **1999**, *299*, 374.
(202) Dubernet, M. L.; Hutson, J. M. *J. Phys. Chem.* **1994**, *98*, 5844.
(203) Manolopoulos, D. E. *J. Chem. Soc., Faraday Trans.* **1997**, *93*, 673.
(204) Meijer, A. J. H. M.; Groenenboom, G. C.; van der Avoird, A. *J. Phys. Chem. A* **1997**, *101*, 7558.

CR990048Z